Interactions of Well-Defined, Pyrene-Functionalized Diblock Copolymers with Single-Walled Carbon Nanotubes

Interactions of Well-Defined, Pyrene-Functionalized Diblock Copolymers with Single-Walled Carbon Nanotubes

BY

CLAIR QI WANG, B.Sc.

A Thesis

Submitted to the School of Graduate Studies

In Partial Fulfillment of the Requirements

For the Degree

Master of Science

McMaster University

MASTER OF SCIENCE (2003) McMaster University

(Chemistry) Hamilton, Ontario

TITLE: Interactions of Well-Defined, Pyrene-Functionalized Diblock Copolymers with Single-Walled Carbon Nanotubes

AUTHOR: Clair Qi Wang, B.Sc.

SUPERVISOR: Professor Alex Adronov

NUMBER OF PAGES: 91

Abstract

Since their discovery in 1991, carbon nanotubes, and especially single walled carbon nanotubes (SWNTs), have attracted significant attention due to their unique structural, mechanical, and electronic characteristics. Although many potential applications for carbon nanotubes have been suggested, several key obstacles currently preclude their practical commercial applications. One of these is their lack of solubility and processability. In order to address this issue, a number of covalent and non-covalent nanotube functionalization techniques have recently been reported in the literature. These methods allow for the manipulation of nanotube properties, such as their solubility, through the attachment of various chemical moieties. Although most of these methods involve covalent attachment of structures to either the ends or sidewalls of SWNTs, several examples of non-covalent functionalization have also been reported. Pyrene, with its flat and aromatic structure, has been shown to form strong π-π stacking interactions with the surface of SWNTs. With this in mind, we explored several methods towards SWNT solubilization with diblock copolymers through non-covalent polymer-nanotube interactions. Living free radical polymerizations (SFRP, ATRP) were employed to produce diblock copolymers with narrow polydispersity. Commercial and synthetic monomers with different functionalities could be utilized to produce polymers with varying properties. Specifically, we used polymers such as

polystyrene, poly(methyl methacrylate), poly(*t*-butyl acrylate) and poly(acrylic acid) as one block of our diblock copolymers. The second block was composed of synthetic pyrene-functionalized monomers mixed with different amounts of monomers that match the composition of the first block. It was found that, upon mixing these diblock copolymers with insoluble nanotubes in various solvents, the nanotubes were partially solubilized through π-π stacking with the pyrene-containing blocks.

Acknowledgements

I would like to convey my gratitude to my research supervisor, Dr. Alex Adronov. With all his effort, I learned not only chemistry from McMaster University, but also English speaking and English writing. Through the two years study accompanied with his untiring support (of course and his criticism), I am becoming a detail-oriented scientist, where the 'detail' indeed is very imperative, either for myself or for a country. I believe he is one of my greatest teachers who always think what I might do better.

My other thanks go to our group, especially: Greg, Zhaoling, Hai, Yuanqin and Matt. Student life is part of our special and precious moment. All of you make my life experience rich and interesting in Canada.

My appreciation also goes to Dr. Stover, Nady and Andy, for the assistance with my experiments.

Another important group is my super-kind family members: my husband Xinyu, daughter Emily, mom and dad. I will get round to cook for you soon honest!

TABLE OF CONTENTS

Page

List of schemes

List of Figures

Page

List of Tables

Chapter 1 Introduction

1.0 Introduction of Single-Walled Carbon Nanotubes

Multi-Walled Carbon Nanotubes (MWNTs) and Single-Walled Carbon Nanotubes (SWNTs) were first discovered by Ijima and coworkers in 1991 and 1993, respectively.[1,2] Since then, carbon nanotubes have attracted much attention due to their unique structural, physical, chemical and electronic properties. However, there are several fundamental obstacles that must be solved before nanotubes can be exploited for many of their envisioned applications.[3] Those challenges include: (1) development of a large scale synthesis, (2) production of purified carbon nanotubes, free of catalyst residues, carbon nanoparticles, and amorphous carbon, (3) separation of the carbon nanotubes according to length, diameter, and chirality (semiconducting from metallic nanotubes), and (4) development of chemical techniques for manipulating nanotube solubility, self-assembly into arrays, and miscibility with various bulk materials.[4-8]

Most chemistry occurs in solution. However, SWNTs are highly insoluble in all known solvents. One factor contributing to this is the strong van der Waals interactions (π-π stacking) that exist between the surfaces of the SWNTs, which allow them aggregate to form intertwined nanotube ropes or bundles.[9] Additionally, the fact that these pseudo-1D sp^2 hybridized carbon atom assemblies do not have any surface functional groups makes them extremely difficult to

dissolve in any media. As a result, a number of research groups around the world have devoted a considerable effort to the development of solubilization strategies. To date, several different approaches have been developed: (a) covalent functionalization at the open ends and defect sites (acid group chemistry); (b) covalent functionalization along the side wall through reactions with the aromatic nanotube structure; (c) supramolecular functionalization (non-covalent functionalization) of SWNTs. Strong evidence showing that functionalized SWNTs can be dissolved in both organic and aqueous media has been reported. The solubility of these functionalized carbon nanotubes makes it possible to characterize, study the properties, and utilize the potential applications of carbon nanotubes using solution-based techniques.

1.1 Structural properties of SWNTs

SWNTs are composed entirely of carbon atoms, forming structures that resemble single sheets of graphene rolled up into seamless cylinders (Figure 1).[2,5] The well-defined cylindrical cavities have a strictly limited diameter, ranging from 0.4 to 4 nm, but vary from microns to multiple centimetres in length, which provides them with a high aspect ratio.[10,11] The diameter as well as the chirality of SWNTs is determined by the lattice vectors (n, m) in the graphene plane (Figure 1). Thus, the lattice vectors are usually used to describe the nanotube properties. For instance, the diameter can be related to the lattice vectors by the equation $d = 0.078 \times (n^2 + m^2 + nm)^{1/2}$ nm (Equation 1), where d is the diameter of a SWNT.

In addition, the chirality (C_h) of SWNTs is defined by the equation $C_h = n \times a_1 + m \times a_2$ (Equation 2), where a_1 and a_2 are unit vectors of the hexagonal honeycomb lattice, and n and m are integers. The chiral vector C_h defines the chiral angle α of a nanotube. For a zigzag tube (n, 0), α equals 0° (Figure 1, b). If $\alpha=30^\circ$ (Figure 1, a), where the nanotube is formed along the line which bisects each hexagon, separating them into two equal parts, then it is an armchair nanotube (n, n). Otherwise, if $0^\circ<\alpha<30^\circ$ (Figure 1, c), it is a chiral tube (n, m).[12]

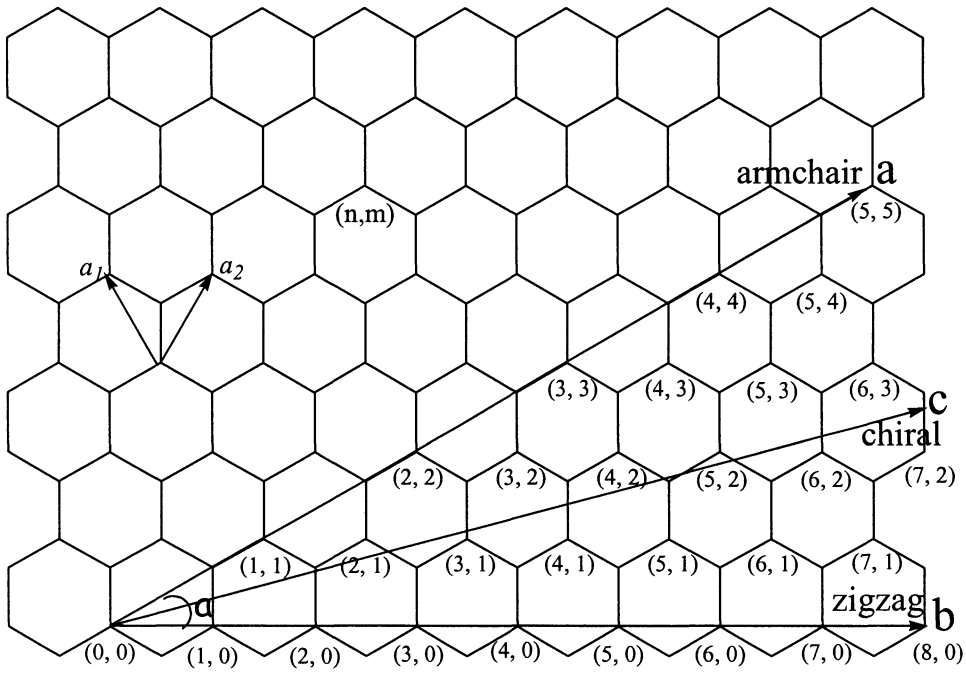

Figure 1. Schematic honeycomb structure of a graphene sheet. SWNTs can be formed by rolling-up the sheet along lattice vectors. The two basis vectors a_1 and a_2 are shown. Folding of the (n, n) and (n, 0) vectors lead to armchair (a) and zigzag (b) tubes, respectively. Folding of the (n, m) vectors lead to chiral tubes (c).

If the value $(n - m)$ is divisible by three (armchair structures), the SWNTs are considered metallic conductors. Otherwise, the nanotubes are semiconductors (chiral and zigzag tubes).[12,13] In addition to their conductivity properties, their tensile strength was measured to be around 1 TPa,[14,15] which is five times stronger than steel. It has also been reported recently that they exhibit a very high thermal conductivity[16] and high mechanical resilience,[17,18] which allows them to be bent without breaking.

1.2 Potential applications of SWNTs

SWNTs show great promise for a variety of applications[19] because of their intrinsic structural robustness, as mentioned above. Their high tensile strength and high mechanical resilience render them useful in high strength materials or as additives for high strength composites (lightweight, high-performance polymer composites). The development of nanoelectronics based on nanotube electronic properties is certainly a most promising area in nanotechnology. Dai and co-workers reported that they measured conductance versus strain and bending angle of individual SWNTs, and found that the electrical and mechanical changes are fully reversible, suggesting potential nanowire-based nanoelectromechanical (NEM) transducers.[20,21] The availability of both semiconducting and metallic nanotubes enables a wide variety of applications. Metallic nanotubes are expected to play an important role as electronic wires (molecular wires), within field emission displays.[22,23] Further, it has been demonstrated that semiconducting

SWNTs can be used as field effect transistors (FETs),[24,25] which are essential components for next-generation computing. It is also established that their conductivity can vary by 2 to 3 orders of magnitude when they are exposed to certain gases, such as ppm level of ammonia (NH_3),[26] nitrous oxide (NO_2),[26] and oxygen (O_2)[27]. These results suggest that SWNTs could possibly be used as miniature chemical or biological sensors,[26-28] as a result of their unique electronic properties.[29]

1.3 Synthesis of SWNTs

Several methods, such as arc discharge,[1,7,30] laser ablation,[6] pyrolysis,[31,32] chemical vapour deposition (CVD),[23,33-35] and high pressure carbon monoxide disproportionation (HiPCO)[36] are utilized for the synthesis of SWNTs. Historically, the first method discovered for the synthesis of hollow SWNTs and MWNTs was the arc discharge method using graphite electrodes in the presence of metal catalysts (Fe, Co, Ni). This process has since been improved and modified to obtain good quantities (grams of nanotubes).[7] Another convenient approach by which carbon nanotubes can be obtained is the pyrolysis of organometallic precursors such as metallocenes and phthalocyanines in a reducing atmosphere. More importantly, aligned nanotube bundles have been obtained from the one-step pyrolysis of organometallics along with other hydrocarbon sources, such as methane and acetylene. In a typical procedure, a heating rate of 50°C/min in the first furnace and an argon flow rate of 1000 sccm have been

employed.[37,38] Alternative routes are based on CVD, in which carbon sources could be acetylene, methane, benzene, carbon monoxide, etc. With one particular method, named the HiPCO process, Smalley's group has described a scalable synthetic technique, where CO is utilized as a feedstock (Equation 3). This is a gas-phase catalytic process where the catalyst (iron-metal clusters) is formed from the pyrolysis of iron pentacarbonyl, $Fe(CO)_5$, at 800°C. Carbon monoxide disproportionates to form solid carbon, which occurs catalytically on the surface of the iron particles, upon which SWNTs nucleate and grow. Compared to other methods, which produce SWNTs in milligram to gram quantities in a few hours, the HiPCO process can produce approximately one kilogram of SWNTs per day. However, some metal catalyst and amorphous carbon remain in the final products, which give a 90% purity and a 40% yield. This process was the source of the SWNTs used in our investigation, which are commercially available from Carbon Nanotechnologies Inc.

$$CO + CO \xrightarrow{\text{Fe-clusters}} CO_2 + C \qquad \text{(Equation 3)}$$

1.4 Covalent Functionalization of SWNTs

It was found previously that shortened SWNTs (s-SWNTs), approximately 100-350 nm in length, could be rendered soluble through covalent functionalization.[39] This chemistry takes advantage of the carboxylic acid groups

formed at nanotube defect sites or open ends as a result of shortening.[40-52] Specifically, amidation and esterification are usually used to attach alkyl chains to SWNTs, thereby improving their solubility. Furthermore, the nanotube-bound carboxylic acid groups have been used to attach a number of other molecules to create novel conjugates. These include the attachment of nanocrystals, biomolecules and organometallic complexes (Figure 2).[40] In addition to the use of pendent carboxylic acid groups, a number of other chemical processes have been demonstrated to work on carbon nanotubes, including [2+1] cycloaddition of nitrenes,[41] hydrogenation via the Birch reduction,[42] fluorination,[43] alkylation,[40] arylation,[44] nucleophilic carbene addition,[41] 1,3-dipolar cycloaddition of azomethine ylides,[45] and the Bingel reaction (cyclopropanation).[46]

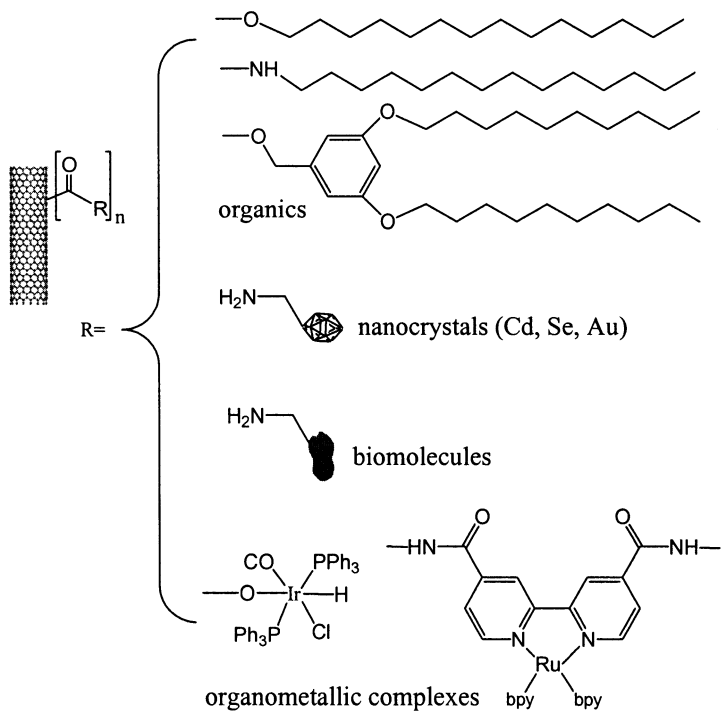

Figure 2. Covalent functionalization of s-SWNTs.

Although covalent functionalization of SWNTs can render the nanotubes soluble and attach different molecules onto their surfaces, it disrupts the ideal aromatic nanotube structure. Therefore, this type of functionalization may impede some of the potential applications of SWNTs. In order to overcome this limitation to the covalent functionalization of SWNTs, non-covalent (supramolecular) functionalization becomes increasingly attractive.

1.5 Supramolecular chemistry

"*Supramolecular chemistry*" is defined as chemistry "beyond the molecule". In contrast to traditional covalent chemistry, supramolecular chemistry is based upon the intermolecular associations, such as non-covalent bonding interactions, that hold two or more building blocks together. On one hand, the concepts of supramolecular chemistry are determined by the nature of the molecular components, and on the other by the type of the interactions that hold them together, including Hydrogen bonding interactions, π-π stacking interactions, hydrophobic interactions, electrostatic interactions, and metal-ligand coordination. In terms of bond strength, van der Waals forces (π-π stacking and hydrophobic interactions) are worth approximately 2 kJ/mol, H-bonding is worth 20 kJ/mol, and an electrostatic interaction is worth 250 kJ/mol, whereas a typical covalent bond strength is much stronger, around 350 kJ/mol. However, the combination of numerous weak interactions could result in a very strong association. Over the past 30 years, noncovalent interactions have increasingly been employed to obtain

well-defined structures through a spontaneous and reversible process, such as the formation of micelles.

Supramolecular chemistry has the advantage of being able to assemble large molecules that combine specific topologies and interesting properties by simply mixing them together. Through recognition-directed association, self-assembly, and self-organization processes, supramolecular chemistry opens new perspectives in materials science that lead to the development of supramolecular materials whose features depend on molecular structure and which involve 'smart' materials, network engineering, and polymolecular patterning.

The self-assembly afforded supramolecular structure is a relatively new and fascinating area in polymer science. By combining the knowledge of organic and synthetic polymer chemistry, many self-assembled structures can be designed and synthesized via intermolecular interactions.

1.6 Supramolecular functionalization of SWNTs

Supramolecular functionalization of SWNTs is particularly attractive because it represents the possibility of attaching various chemical moieties to SWNTs without disrupting the ideal nanotube bonding network, thus retaining the useful properties of SWNTs. There are several research groups addressing this issue using different approaches, which may roughly be divided into four categories: the use of small molecules with flat, aromatic structure, such as pyrene[53] (π-π stacking), the use of surfactants[54] (hydrophobic interactions), the

use of electrostatic interactions,[55] and the use of polymers[56-61] as solubilizing agents.

In the first category, a series of pyrene derivatives have been shown to exhibit strong interactions with SWNTs, allowing not only for the solubilization of the nanotubes, but also for the surface modification of SWNTs. For example, nanotubes functionalized with 4-pyren-1-yl-butyric acid 2,5-dioxo-pyrrolidin-1-yl ester via π-stacking can be reacted with protein through amidation, to give a protein/SWNT conjugate (Figure 3).[62]

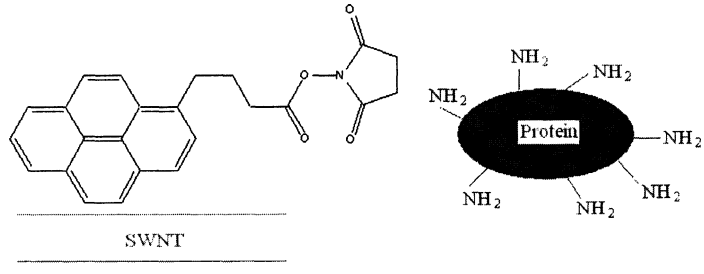

Figure 3. Schematic diagram of 4-pyren-1-yl-butyric acid 2,5-dioxo-pyrrolidin-1-yl ester/SWNT and protein.

For the use of electrostatic interactions, Haddon's group[55] reported a method that could solubilize the full-length SWNTs (average length >1 μm) in many common organic solvents. This involved a one-step exfoliation by supramolecular (electrostatic) functionalization between an octadecylammonium and the carboxylic acid groups present in the purified SWNT ropes. Comparing to the soluble shortened nanotubes, soluble full-length SWNTs are preferred due to their higher aspect ratio, less tedious preparation and easier to scale up at a low cost.

In the last category, several polymers have been reported to effectively solubilize carbon nanotubes. It has been shown that these polymers are reasonably flexible and can wrap themselves either around SWNTs or around ropes of nanotubes and disrupt the van der Waals interactions that cause SWNTs to aggregate into bundles. For example, Blau and co-workers showed that the block copolymer, poly(*p*-phenylenevinylene-*co*-2,5-dioctyloxy-*m*-phenylenevinylene) (PmPV-*co*-DOctOPV) could wrap and solubilize SWNTs.[56-61] Smalley's group reported using water-soluble polymers, including poly(vinylpyrrolidone) (PVP) and polystyrene sulfonate (PSS) to reversibly solubilize SWNTs in water.[63] SWNT complexes with poly{(*m*-phenylenevinylene)-*co*-[(2,5-dioctyloxy-*p*-phenylene)vinylene]} (PmPV) and poly{(2,6-pyridinylenevinylene)-*co*-[(2,5-dioctyloxy-*p*-phenylene)vinylene]} (PPyPV) have gained attention recently for not only providing solubilized nanotubes, but also for their utilization in the fabrication of light-emitting diodes.[64,65] Other macromolecules, having the same kind of PmPV-like structure, with more rigid and well-defined characteristics, would be expected to be even more efficient at breaking up nanotube bundles via either threading themselves onto or clipping themselves around SWNTs. Following this idea, Heath and coworkers utilized a one-step polymerization which generated a hyperbranched alternative of the PmPV conjugated copolymer (Figure 4) and reported its ability to solubilize SWNTs by breaking up the nanotube bundles via threading themselves around SWNTs.[66] Similar to the highly conjugated and hyperbranched polymer just mentioned, non-dipolar

dendrimeric polyphenylenevinylenes (PPV's), also called stilbenoid dendrimers, have been shown to effectively increase the solubility of shortened nanotubes through π-π stacking interactions.[67-70] These homogeneous, supramolecularly functionalized, nanotube-based polymers would possibly allow the investigation in the formation of fibres, films, and coatings.

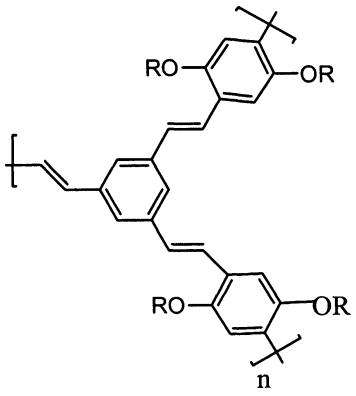

Figure 4. Hyperbranched polymer used for supramolecular functionalization of s-SWNTs.

1.7 Well-defined block copolymers

Macromolecules, such as well-defined block copolymers, have been widely employed in supramolecular chemistry. By covalently linking the polymer segments with different physical properties, new materials exhibiting new and useful characteristics can be created. For example, diblock and triblock copolymers with different solubility characteristics have been studied for their ability to self-assemble in solution to afford stable nanoscale particles.[71,72] Such complex nanostructures have shown promising applications in environmental,

biomedical, and materials fields, such as the removal of pollutants, drug delivery, gene therapy, and coatings.[73-75]

The crucial factor in each of the supramolecular assemblies mainly depends on the nature of the block copolymers, their molecular weight, and their different compositions. To achieve well-defined block copolymers, living free-radical polymerizations have recently been introduced as a facile method for their preparation.

1.8 Living free radical polymerizations (LFRP)

Living polymerizations are one of the most advanced synthetic methods in the field of polymer science. Ionic living polymerizations are already well established for making materials with well-defined architecture, including controlled molecular weight and narrow polydispersity.[76,77] However, ionic living polymerization is limited by the demanding nature of the experimental setup. For this reason, in recent years, there has been growing interest in the use of living radical polymerizations, which offer the control of a living polymerization without the associated demanding experimental conditions. Additionally, LFRP is applicable to a wide range of monomers. Nitroxide-mediated Stable Free Radical Polymerization (SFRP),[78-80] Atom Transfer Radical Polymerization (ATRP),[81-85] and Reversible Addition Fragmentation Transfer Polymerization (RAFT)[86-89] are versatile methods for living radical polymerizations. They have been widely used for the synthesis of well-defined block, gradient, and alternating copolymers.[90-93]

1.8.1 SFRP

Nitroxides such as 2,2,5,5-tetramethyl-3-(1-phenylethoxy)-4-chloromethyl-phenyl-3-azahexane,[94] compound **1**, thermally decompose (Scheme 1) at 125°C to form carbon-centered free radicals (initiating radicals) and oxygen-centered free radicals, 2,2,5,5-tetramethyl-4-phenyl-3-azahexane-3-nitroxide, compound **2** (alkoxyamine derivatives). The oxygen-centered free radicals are essentially stable and will not participate in the polymerization further, thus acting as radical traps.

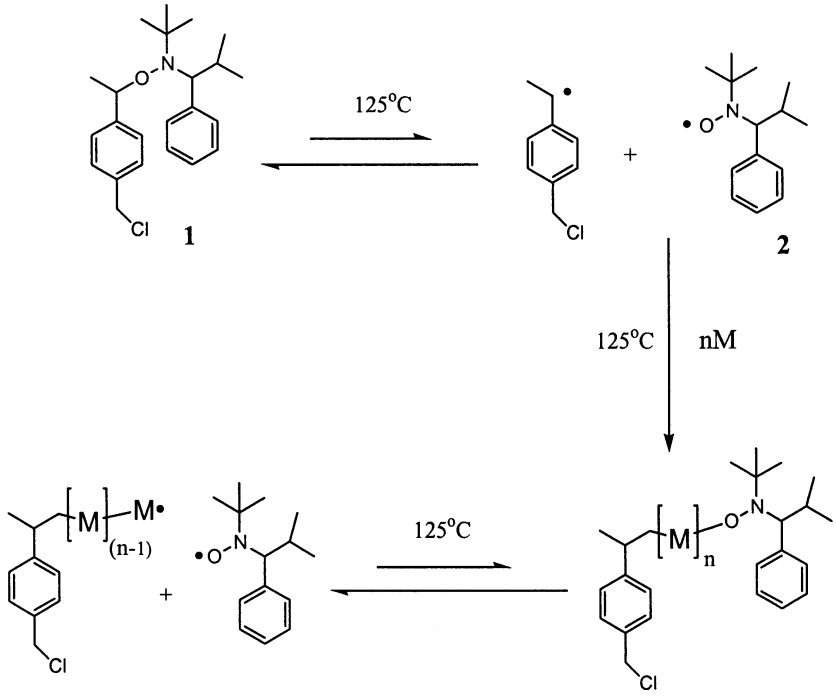

Scheme 1. General mechanism for 2,2,5,5-tetramethyl-3-(1-phenylethoxy)-4-chloromethyl-phenyl-3-azahexane **1** initiated SFRP

Some additives, such as acetic anhydride and stable free nitroxide radicals (the radical to which the corresponding initiator will thermally decompose) are

normally used to obtain a faster polymerization rate and narrower polydispersity.[95,96] The family of nitroxides[92] permits the polymerization of a wide variety of monomers: acrylates, acrylamides, 1,3-dienes and acrylonitrile. However, to date, styrenics are still the easiest monomer family to be polymerized under SFRP in a living manner.

1.8.2 ATRP

A successful ATRP is accomplished through fast initiation and rapid, reversible deactivation, where all the chains grow uniformly. A general mechanism for ATRP is shown in Scheme 2. The reaction is catalyzed by a transition metal complex (M_t^n-Y/Ligand, where M_t^n is a transition metal and Y is a halogen atom) through a reversible redox process. It is a one-electron oxidation with simultaneous abstraction of a halogen atom, X, affording a dormant species, R-X. The atom transfer is the key step for the uniform growth of the polymeric chains. This process occurs with a rate constant of activation, k_{act}, and deactivation k_{deact}. The addition of the vinyl monomers to the active radicals to form polymer chains is similar to a conventional radical polymerization with the rate constant of propagation k_p. Termination reactions (k_t) also occur in ATRP, mainly through radical coupling and disproportionation. However, in a well-controlled ATRP, less than a few percent of the polymer chains would undergo termination reactions. The generated oxidized metal complexes, X-M_t^{n+1}-Y, act as

the persistent radicals to reduce the stationary concentration of growing radicals and thereby minimize the contribution of termination.

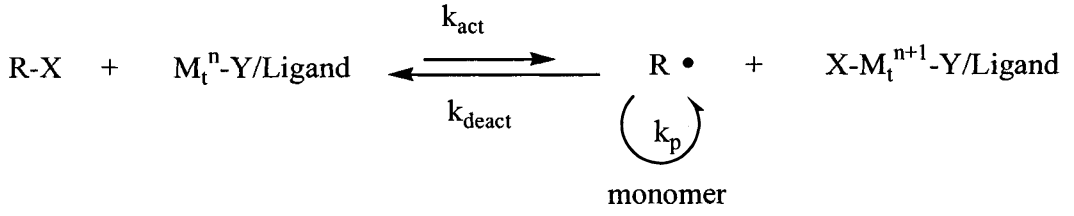

Scheme 2. General mechanism for transition-metal-catalyzed ATRP

Typical monomers for ATRP include styrenes, (meth)acrylates, (meth)acrylamides, and acrylonitrile, where the substituents can stabilize the propagating radicals. Alkyl bromides and chlorides are typically used as the initiators, as they have been found to promote rapid initiation and excellent molecular weight control. A variety of transition metal complexes have been utilized as ATRP catalysts, including Copper (Cu), Ruthenium (Ru), Iron (Fe) and Rhenium (Re).[91] So far, the majority of the work has been reported using the copper based systems. ATRP can be carried out in bulk, in solution, or in a heterogeneous system (e.g., emulsion, suspension). Various solvents, such as benzene, toluene, anisole, diphenyl ether, dimethyl formamide (DMF), alcohol, water, and many others, have been used for different monomers. The polymerization temperature depends mostly on the monomer, the catalyst, and the desired molecular weight.

Chapter 2 Objectives

Our study aims to improve the solubility properties of SWNTs via supramolecular functionalization, which offers the opportunity of attaching various molecules to SWNTs without disrupting their ideal conjugated structure. Pyrene, with its flat and aromatic structure, has been shown to form strong π-π stacking interactions with the surface of SWNTs. We want to take advantage of this known interaction to solubilize nanotubes in organic or aqueous solutions, with the use of pyrene-functionalized diblock copolymers. As mentioned in section 1.5, the critical element in each of the supramolecular assemblies depends not only on the type of the interactions that hold them together, but also on the nature of the two components. For a successful solubilization of SWNTs, the nature of the other component, the diblock copolymer (the molecular weight and its composition) is another crucial factor. Thus, we focused on soluble diblock copolymers in which one block is designed to increase the solubility, and the other block contains pyrene that could self-assemble with SWNTs, in the hope of forming a soluble polymer-SWNT conjugate (Figure 5).

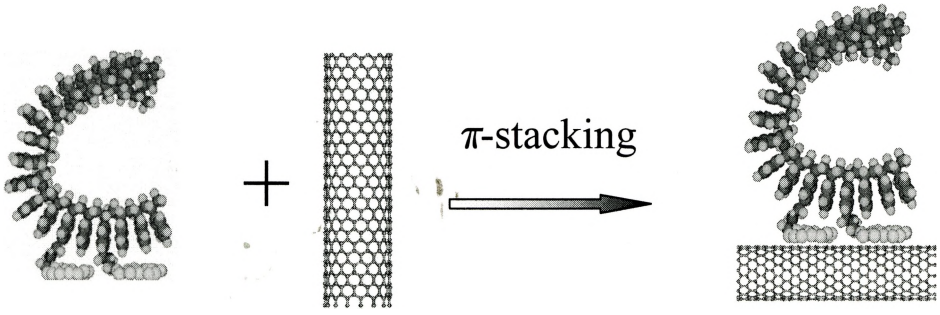

Figure 5. The formation of the polymer-SWNT conjugate.

Thus, another objective of this thesis is to synthesize these novel diblock copolymers, as described in Figure 6. The polymers employed in our investigation are polystyrene (PS), poly(methyl methacrylate) (PMMA), poly(*t*-butyl acrylate) [P(*t*-BA)], and poly(acrylic acid) (PAA), as the first block in our diblock copolymers. The second block was composed of synthetic pyrene-functionalized monomers mixed with different amounts of monomers that match the composition of the first block. Figure 6 schematically depicts two types of the designed diblock copolymers. The first of these is composed of only pyrene containing monomers within the 2nd block (Figure 6, a). The other contains two components in the second block (Figure 6, b). Various monomers in the first block and different components in the second block provide the chance to optimizing the solubility of nanotubes, depending on which polymer is used and how much pyrene is incorporated into each polymer.

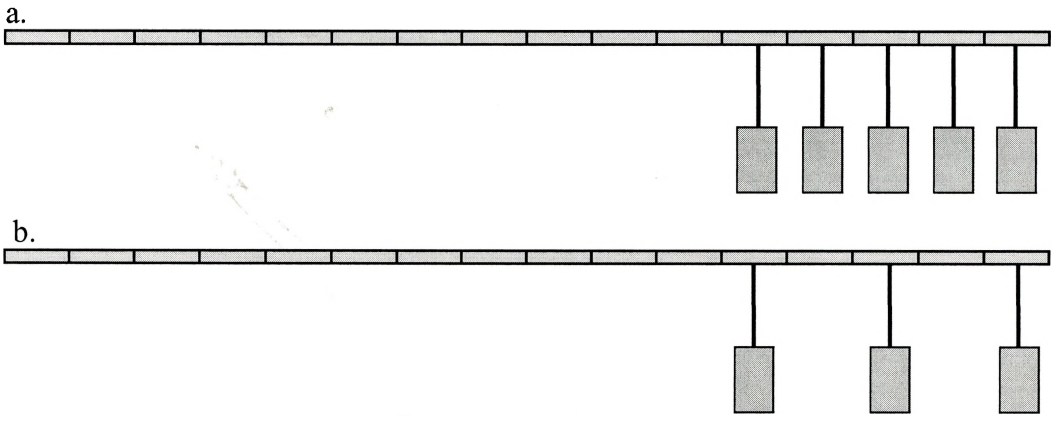

Figure 6. Schematic diagram of the designed diblock copolymers: (a) feed ratio of pyrene derivative to the other monomer in the 2nd block was 100:0 (The second block only has pyrene inside); (b) feed ratio of pyrene derivative to the other monomer in the 2nd block was 40:100 or 10:100 (pyrene was diluted with the same monomer used in the 1st block).

Shortened SWNTs (s-SWNTs) were chosen because they are much easier to dissolve through chemical functionalization than unshortened SWNTs according to the literature.

Chapter 3 Results and discussion

3.0 Overview

As discussed in the objectives, diblock copolymers composed of segments of styrene, MMA, *t*-BA, or acrylic acid coupled with pyrene segments of functionalized monomers were selected as the starting points for the preparation of polymer-SWNT composites to increase the solubility of shortened SWNTs (s-SWNTs). The synthetic design involved four basic concepts: (1) synthesis of polymerizable pyrene derivatives (styrene-pyrene monomer and acrylate-pyrene monomer); (2) preparation of the PS series (styrene with styrene-pyrene) of diblock copolymers by a sequential SFRP method; (3) preparation of the PMMA or P(*t*-BA) series (acrylates with acrylate-pyrene) of diblock copolymers by a sequential ATRP process; (4) the selective cleavage of the *tert*-butyl ester functionalities to form a water soluble (amphiphilic) diblock copolymer, the PAA series (acrylic acid with acrylate-pyrene). The GPC measurement of synthesized homopolymers and block copolymers provided the molecular weight characteristic and evidence of block copolymer formation. ^{1}H NMR analysis provided information about both the molecular weight and the composition of the resulting polymers.

The supramolecular functionalization of the s-SWNTs with each of the synthetic diblock copolymers was done by sonication in THF or water at room

temperature. The resulting stable polymer-SWNT solutions have been observed for six months. The solubility of the functionalized s-SWNTs was measured by UV-Vis spectroscopy according to Smalley's method.[97]

3.1 Synthesis and characterization of pyrene monomers

As mentioned in the objectives, the second block of the designed diblock copolymer was composed of synthetic pyrene-functionalized monomers mixed with different amounts of monomers that match the composition of the first block. In order to ensure that the living free radical polymerizations occur smoothly, it is necessary for the two monomers to have similar reactivity ratios. We therefore chose to prepare two polymerizable pyrene derivatives that mimic the structure of the co-monomer. The first of these was a styrene derivative, styrene-pyrene, and the second was an acrylate derivative, acrylate-pyrene. The styrene-pyrene monomer was used to prepare poly[styrene-co-(styrene-pyrene)], and the acrylate-pyrene monomer was used to prepare poly[acrylate-co-(acrylate-pyrene)]. Each of these is discussed separately in the following sections.

3.1.1 Synthesis and characterization of the styrene-pyrene monomer

Styrene-pyrene monomer **5** was obtained as shown in scheme 3. Refluxing 4-vinylbenzyl chloride **4** in a mixture of 1-pyrenebutyric acid **3**, 18-crown-6, and potassium carbonate in acetone for 4 hours led to the formation of monomer **5**. The reaction was monitored by thin layer chromatography (TLC) and the final

product was purified by column chromatography using CH_2Cl_2/Hexanes 6/4 as the eluent. After drying under vacuum overnight, a yellow powder (93% yield) was obtained.

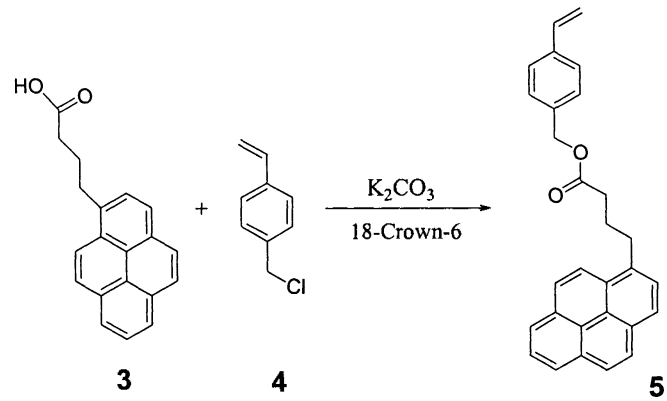

Scheme 3. Synthesis of styrene-pyrene monomer **5**

Having obtained the styrene-pyrene monomer **5**, ^1H NMR, ^{13}C NMR, and mass spectrometry were utilized to characterize the product. In Figure 7 (^1H NMR), the signals at 2.24, 2.52, 3.39 and 5.15 ppm correspond to the eight methylene protons. Three vinyl protons appear at 5.28, 5.76 and 6.74 ppm. The signals in the range of 7.81 to 8.29 ppm correspond to the nine pyrene protons. The integrated area of the resonance peak of the four benzene protons, nine pyrene protons, eight methylene protons and three vinyl protons are all consistent with the structure. Monomer **5** showed signals at 115-140 ppm for the sp^2 carbons in ^{13}C NMR (Figure 8). The resonance at 174.5 ppm is characteristic for the C=O moiety. The signals at 28.0, 33.9, 35.1, and 67.2 ppm are diagnostic for the methylene carbons. Mass spectrometry (Figure 9) gives a molecular weight of

404.2 Da, exactly matching the expected molecular weight of monomer **5**. These results indicate that desired styrene-pyrene has been obtained.

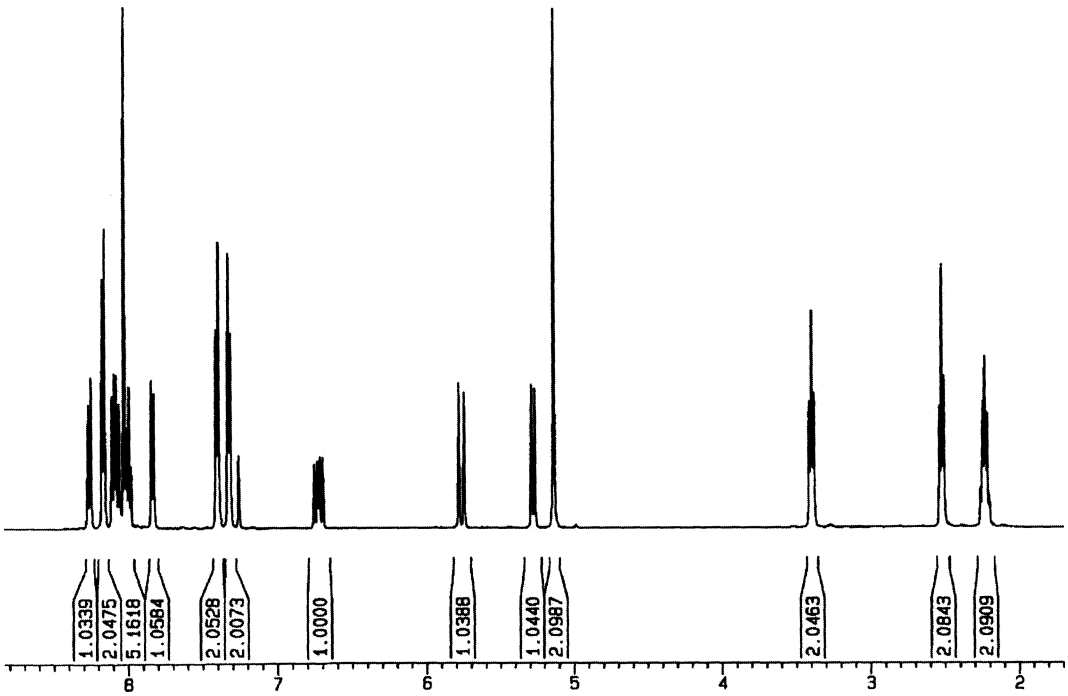

Figure 7. ^{1}H NMR spectrum of monomer **5** in $CDCl_3$.

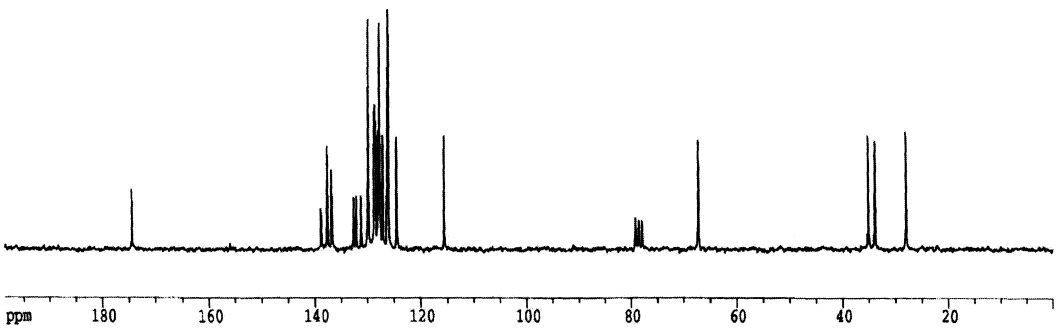

Figure 8. ^{13}C NMR spectrum of monomer **5** in $CDCl_3$.

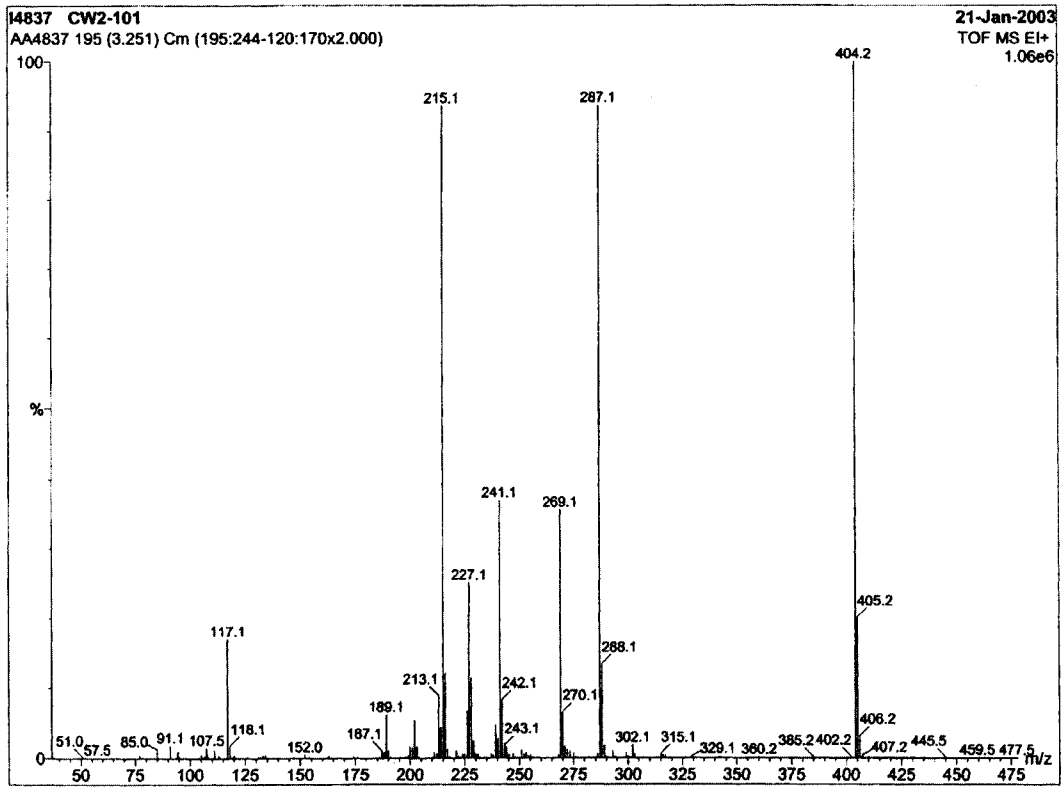

Figure 9. Mass spectrum of monomer **5**.

3.1.2 Synthesis and characterization of acrylate-pyrene monomer

Scheme 4 illustrates the synthetic route to the acrylate-pyrene monomer **8**. Addition of acryloyl chloride **7** to 1-pyrenebutanol **6** in the presence of triethylamine led to the formation of acrylate-pyrene monomer **8**. The reaction was monitored by TLC and purified by column chromatography using pure dichloromethane (DCM) as eluent. After drying under vacuum overnight, a yellow powder was obtained (90% yield).

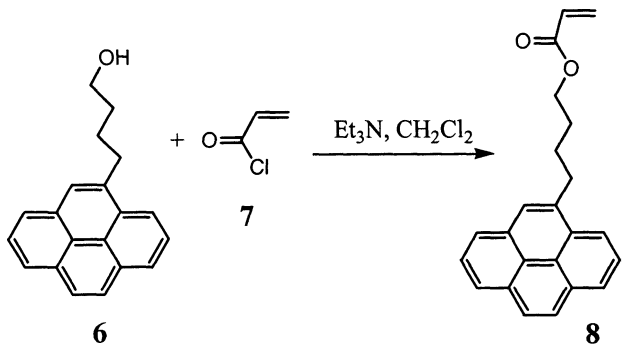

Scheme 4. Synthesis of acrylate-pyrene monomer **8**

Having obtained monomer **8**, ^{1}H NMR, ^{13}C NMR, and mass spectrometry were used to characterize the product. In Figure 10 (^{1}H NMR), the peaks at 7.78-8.32 ppm are assignable to the protons of the aromatic structure. The signals at 1.91, 3.37, and 4.26 ppm correspond to the eight methylene protons. Three vinyl protons appear at 5.82, 6.16 and 6.44 ppm. The integrated area of the nine pyrene protons, eight methylene protons and three vinyl protons are all consistent with the structure. Monomer **8** showed 123-137 ppm signals for sp^2 hybridized carbons in the ^{13}C NMR (Figure 11). The resonance at 166.1 ppm is characteristic for the C=O moiety. The signals at 27.8, 28.3, 32.7, and 64.2 ppm are diagnostic for the methylene carbons. Mass spectrometry (Figure 12) gives a molecular weight of 328.1 Da, consistent with the calculated molecular weight of monomer **8**. These results suggest that desired acrylate-pyrene monomer was obtained.

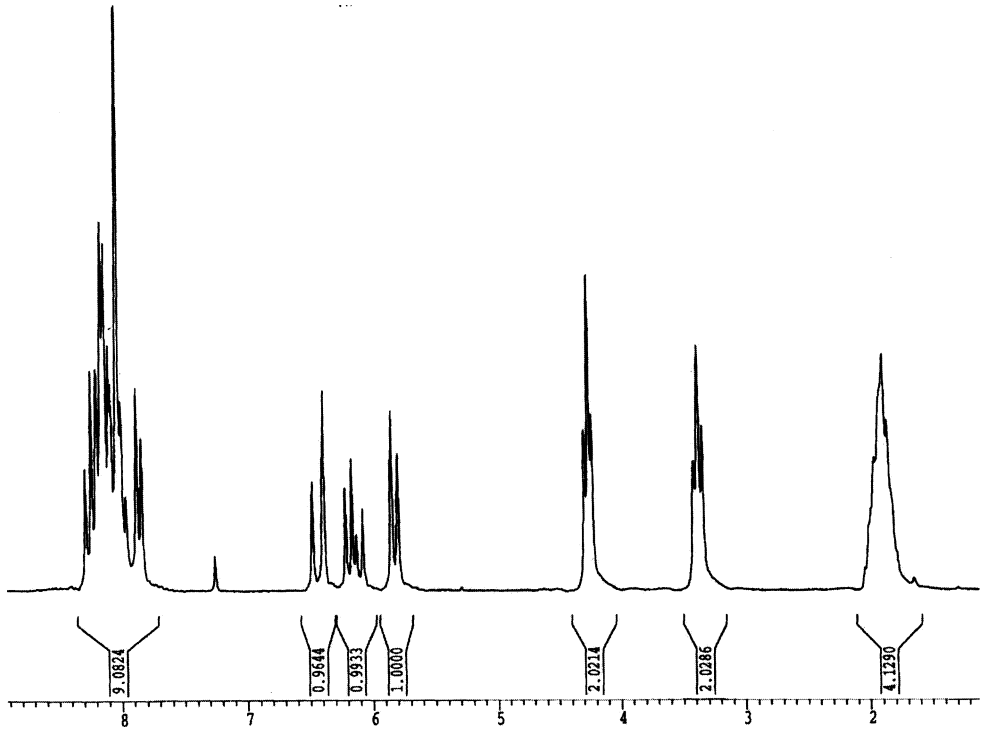

Figure 10. ^{1}H NMR spectrum of monomer **8** in $CDCl_3$.

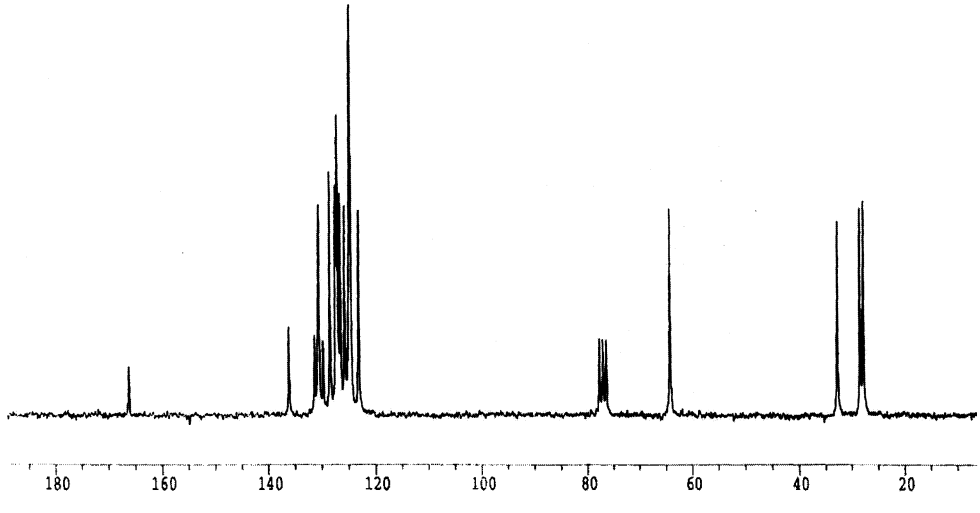

Figure 11. ^{13}C NMR spectrum of monomer **8** in $CDCl_3$.

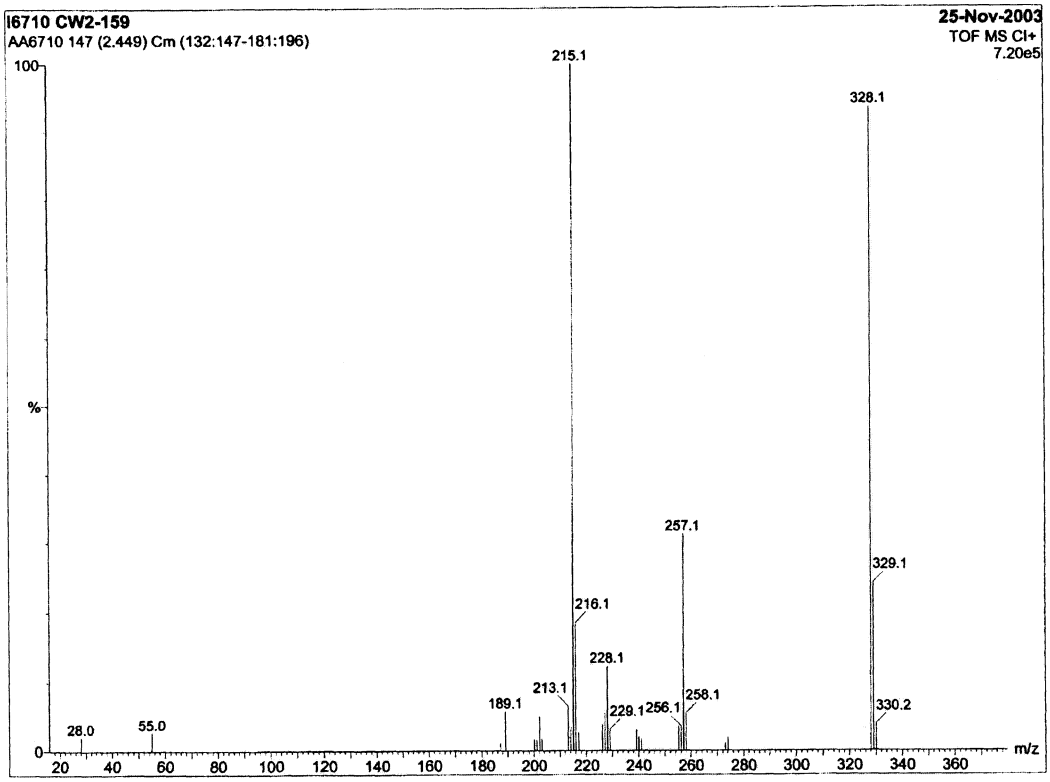

Figure 12. Mass spectrum of monomer **8**.

3.2 Polymerization and characterization

3.2.1 Preparation and characterization of the PS series of polymers

Nitroxide-mediated SFRP is a convenient living polymerization method, especially for styrenics. Compound **1** (2,2,5,5-tetramethyl-3-(1-phenylethoxy)-4-chloromethyl-phenyl-3-azahexane) was used as the initiator and the free nitroxide radical **2** (2,2,5,5-tetramethyl-4-phenyl-3-azahexane-3-nitroxide) was used as an additive to help control the polymerization (Scheme 5). Both **1** and **2** were synthesized following the procedure reported by Hawker and co-workers.[94] Additionally, acetic anhydride was used as another additive for SFRP to obtain a

relatively fast polymerization rate and narrow polydispersity.[95,96] The polymerizations were performed in chlorobenzene at 125°C. The polymer samples were isolated and purified by precipitation into methanol and dried under vacuum for three days.

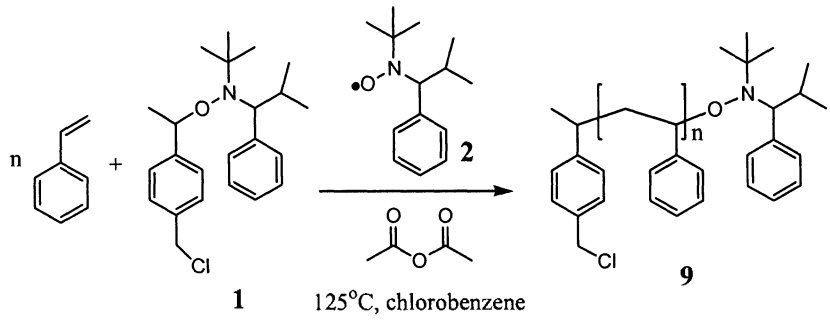

Scheme 5. Homopolymerization of PS by SFRP

Our first experiments were focused on determining whether the SFRP of styrene could be carried out in a living manner. In order to address this issue, two different techniques were utilized to obtain information on the livingness of the polymerization. The first one involved monitoring the polymerization by Gel Permeation Chromatography (GPC) at various reaction times. Figure 13 displays the resulting GPC curves, and clearly shows that the molecular weight of PS increased cleanly with the polymerization time. The plots of the molecular weight (Mn) and polydispersity (PDI) of the polymer versus reaction time for the solution polymerization of styrene are presented in Figure 14. It illustrates more clearly that the molecular weight of polystyrene increased linearly as a function of polymerization time, and polydispersity decreased from 1.28 after the first half

hour to 1.08 after 6.5 hours. Both Figures 13 and 14 indicate that a controlled polymerization of styrene has been achieved using nitroxide **1** as the initiator.

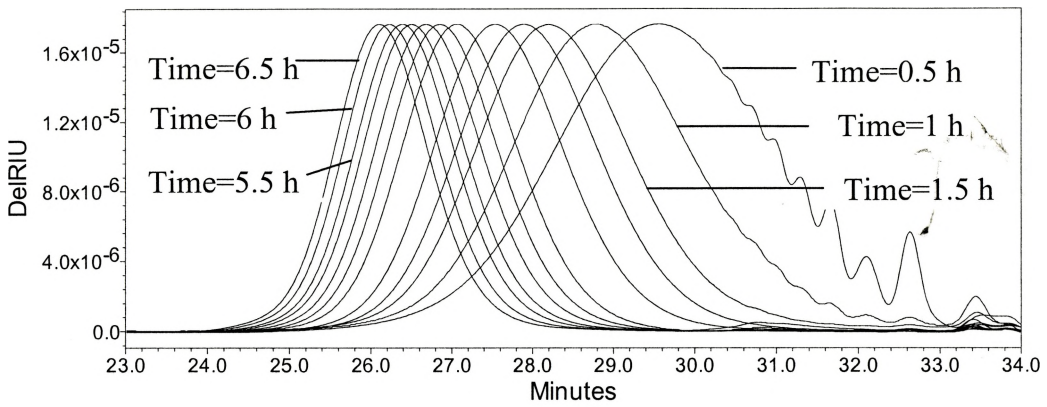

Figure 13. GPC traces of polystyrene at various polymerization times.

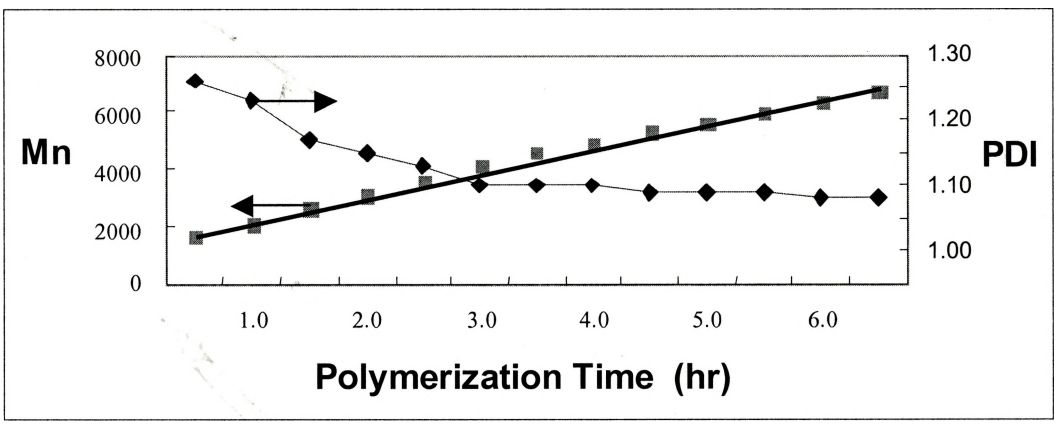

Figure 14. Plots of molecular weight (■) and polydispersity (◆) versus polymerization time for the solution polymerization of styrene.

The other method applied to test the livingness of polystyrene synthesized by SFRP was done by chain extension, as exhibited in Scheme 6. The nitroxide end group of the synthesized polymer can be dissociated at 125°C, resulting in a

radical chain end on the polymer that can be used to react with additional monomers. Figure 15 displays the GPC curves of chain extension product **10** (Mn=45000, PDI=1.1) and the starting material **9** (Mn=5000, PDI=1.2), indicating successful chain extension with styrene. Both of the two methods show that the polystyrene synthesized by SFRP is a living polymer, and could be used as a macroinitiator to polymerize other vinyl monomers.

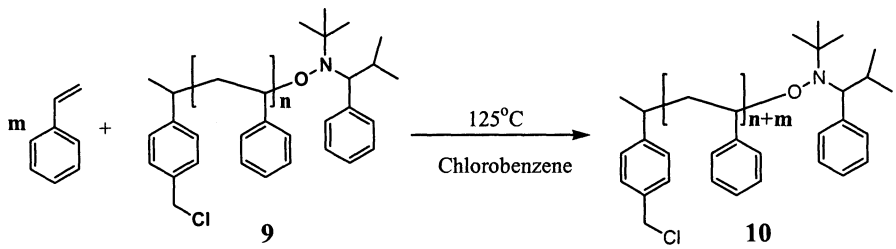

Scheme 6. Chain extension of PS

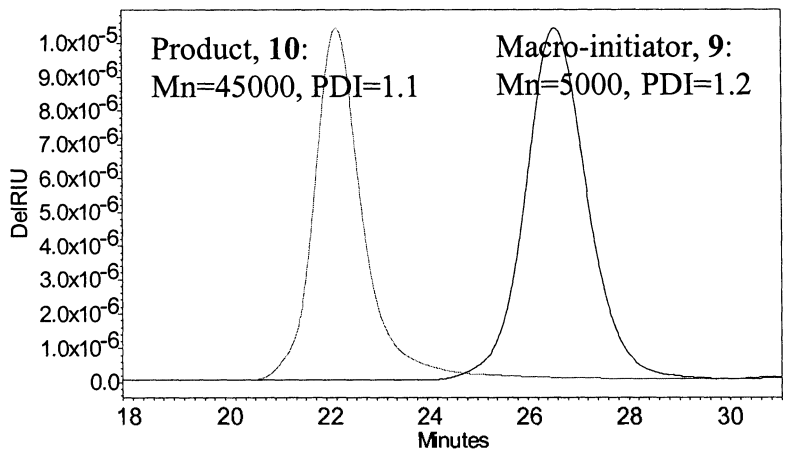

Figure 15. GPC traces of PS, as a macroinitiator **9** and as a chain extension product **10**.

Preparation of the macroinitiator, PS

Knowing that PS obtained via SFRP retains living characteristics, polymerization of styrene in chlorobenzene at 125°C using nitroxide **1** as the initiator was performed at a 150:1 molar ratio of styrene:**1**. The polymerization time applied was 16 hours, and the final product (**11**) was analyzed by both GPC (Mn=13,000, PDI=1.08) and NMR measurements. Based on the ^{1}H NMR spectrum of **11** (Figure 16, a), it is possible to determine the polymer molecular weight by comparing the integration of signals corresponding to the initiator and the polymer backbone. The resonance at 4.65 ppm is assignable to the methylene group of the initiating chain end. The main peaks at 1.2-2.5 ppm and 6.2-7.4 ppm are assignable to the methine, methylene, and phenyl protons of the polystyrene chain. The molecular weights calculated from NMR and measured from GPC are reasonably close, but not identical (Table 1). These observed difference is due to the fact that both measurements are prone to errors; the GPC method is a relative comparison based on calibration curve, whereas the NMR method relies on accurate measurement of the area under a very small peak. Nevertheless, the reasonable agreement between the two methods allowed us to arrive at some conclusions about the overall composition of the different polymers.

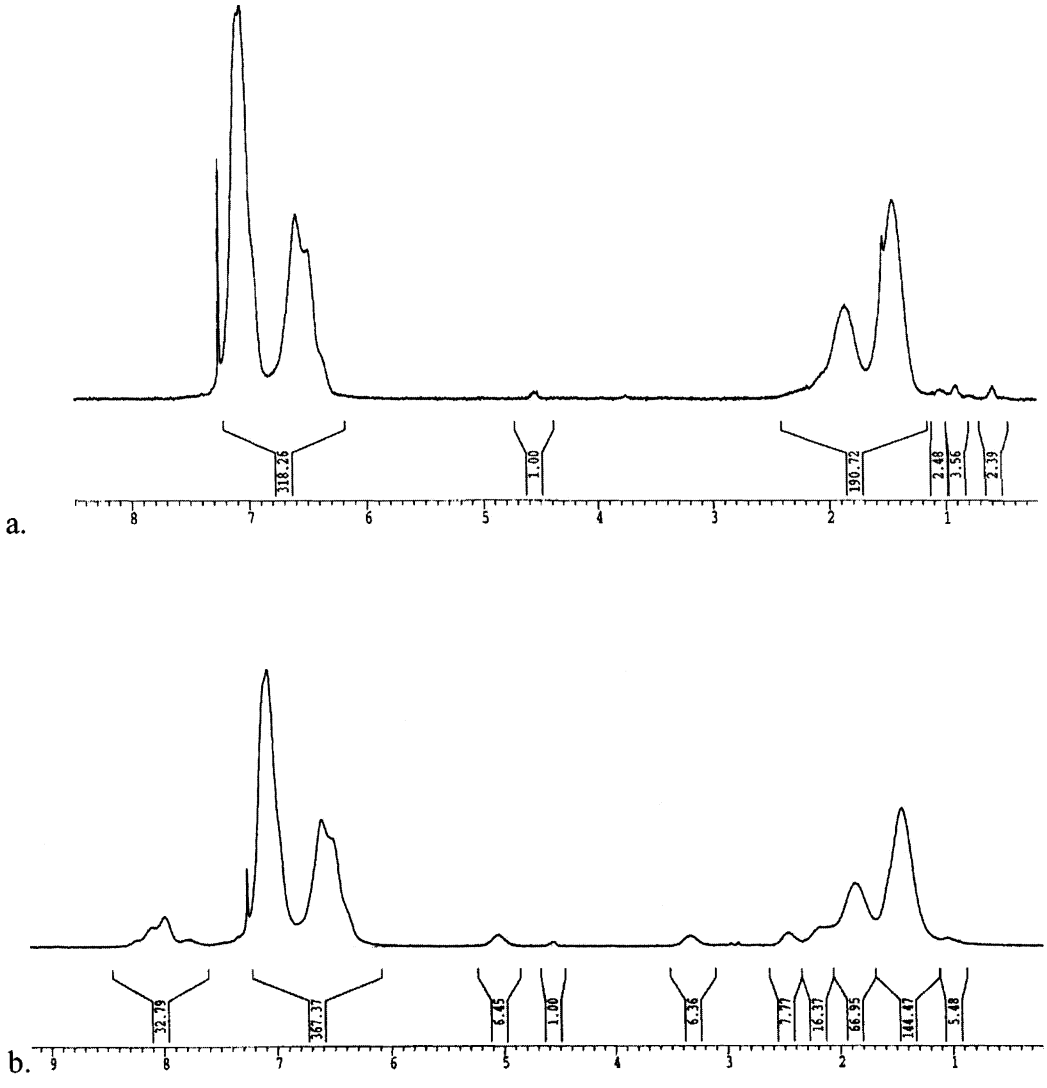

Figure 16. ^{1}H NMR spectra of (a) PS **11** and (b) block copolymer **13**.
(**12**, **13**, and **14** have a similar ^{1}H NMR spectrum)

Table 1. Characteristics of the PS series of diblock copolymers

Polymer	Feed Ratio of the 2nd block (p:m)	n (NMR[a]) (unit)	p (NMR[a]) (unit)	m (NMR[a]) (unit)	Mn NMR[a]	Mn GPC[b]	PDI GPC[b]
11	0	126	0	0	13,000	11,500	1.08
12	100:0	126	9	0	16,500	13,000	1.18
13	40:100	126	6	12	16,800	13,500	1.22
14	10:100	126	5	34	18,500	16,500	1.18

[a]Determined by ^{1}H NMR spectroscopy comparing the integration of initiator **1** signal at 4.65 ppm to the signal of the polymer at 6.2-7.4 and 3.3 ppm. [b]Determined using polystyrene standards.

Preparation and characterization of the PS series of diblock copolymers

Polystyrene (PS) has served as the macro-initiator for the formation of poly[styrene-*b*-(styrene-pyrene)] **12** and poly{styrene-*b*-[(styrene-pyrene)-*r*-styrene)]} (**13** and **14**), collectively named the PS series of diblock copolymers. They were obtained by polymerizing the mixture of monomer **5** and styrene at three different molar ratios (100:0, 40:100, and 10:100 of **5** to styrene, respectively) in chlorobenzene at 125°C using the polymer **11** as the macroinitiator (Scheme 7). For all the reactions, the polymerization time was 16 hours.

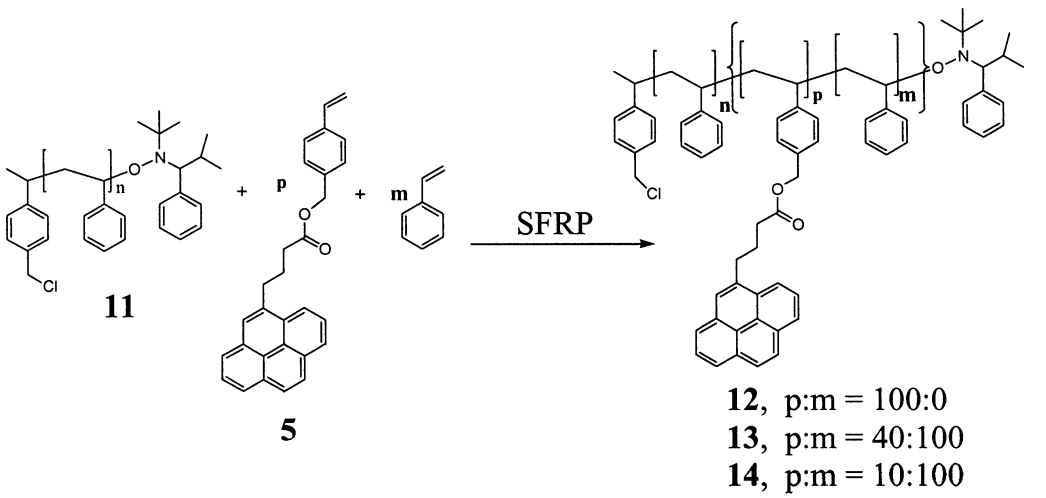

Scheme 7. Preparation of the PS series of diblock copolymers

Figure 16 displays the ^{1}H NMR spectra of pure PS **11** (Figure 16, a) and one of the three synthesized copolymers, **13** (Figure 16, b). All of the three copolymers composed of styrene and monomer **5** have a similar NMR spectrum, except for the integration of the peaks attributed to the second block. Indeed, the copolymer composition can be obtained by comparison of the integrated area of the peak corresponding to the polymer backbone protons or the aromatic protons, the pyrene protons, and the proton in the chloromethyl position of the initiator. The comparison of the two spectra, Figure 16 (a) and Figure 16 (b), illustrates that pyrene monomer **5** has been successfully incorporated into the block copolymers. The molecular weight and the composition of the copolymers calculated from NMR are listed in Table 1.

Figure 17 presents the GPC traces of the three synthesized diblock copolymers (**12, 13,** and **14**) and their macroinitiator (**11**). The difference between the number-average molecular weight of the copolymer and that of the macroinitiator gives the length of the second block. As can be seen from Figure 17, a clean shift of the entire molecular weight distribution to the higher molecular weight region of all three copolymers is observed, suggesting that the copolymers were obtained in a controlled manner. The GPC traces of copolymer **12** and **14** showed a small shoulder, which indicates some termination (possibly by radical coupling) between polymers has happened. The molecular weight and polydispersity data obtained from GPC is also listed in Table 1.

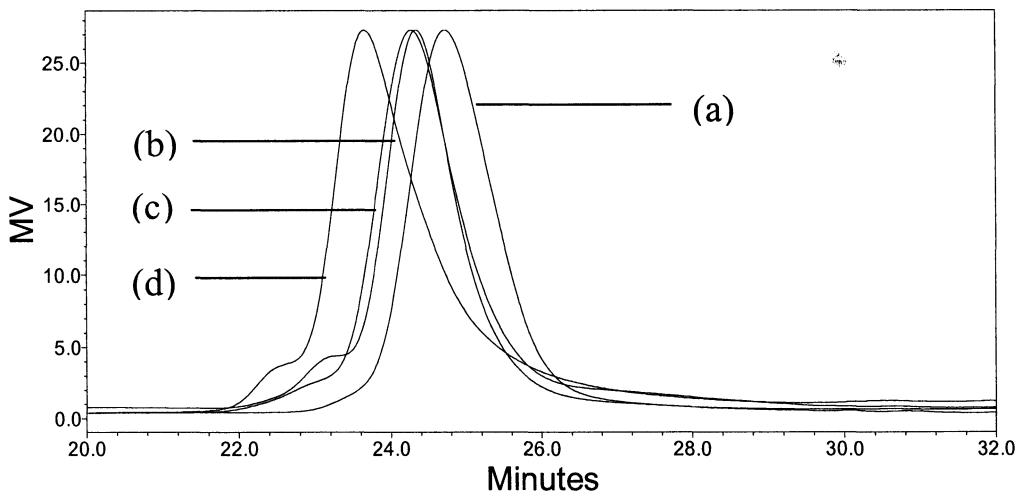

Figure 17. Comparison of GPC traces for (a) the PS **11**, macroinitiator; (b) Poly[styrene-b-(styrene-pyrene)] diblock copolymer, **12** (p:m=100:0); (c) Poly{styrene-b-[(styrene-pyrene)-r-styrene]} diblock copolymer, **13** (p:m=40:100); (d) Poly{styrene-b-[(styrene-pyrene)-r-styrene]} diblock copolymer, **14** (p:m=10:100).

As pyrene is fluorescent, GPC analysis with a fluorescence detector was also employed to ensure that pyrene has been successfully incorporated into the second block. Figure 18 displays the fluorescence chromatograms of the PS series of polymers as a function of elution time. For this analysis, the excitation wavelength was 350 nm and emission wavelength was 450 nm. All three copolymers showed significant fluorescence where pure PS showed no fluorescence. The samples of three block copolymers prepared for this analysis were more than ten times more dilute than the samples prepared for analysis with the RI detector. The fluorescence peaks (Figure 18) of these three copolymers match up well with the RI traces (Figure 17), which indicate that all of the three different diblock copolymers have incorporated monomer **5** into them. All of these measurements confirmed that the designed PS series of diblock copolymers were prepared.

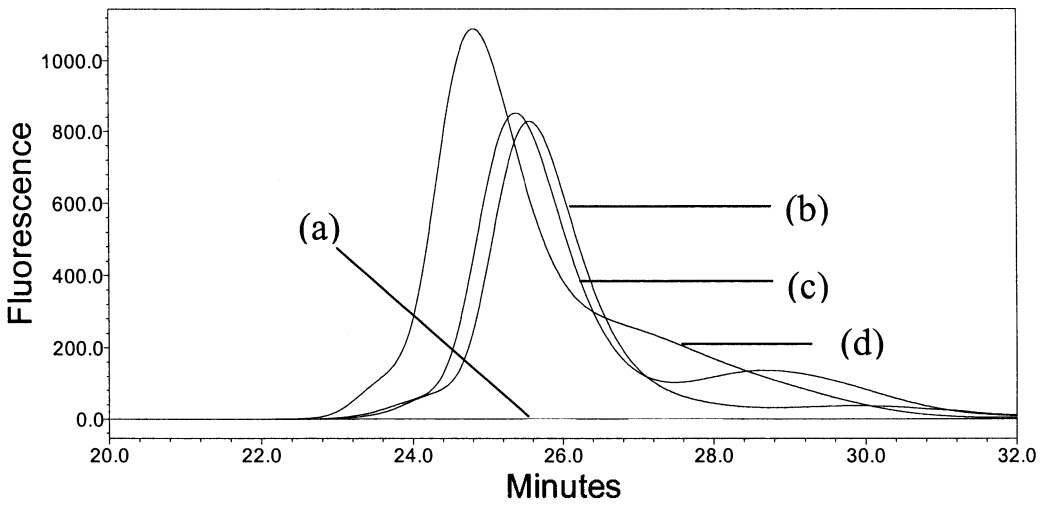

Figure 18. Comparison of fluorescence curves for (a) the PS **11**, macroinitiator; (b) diblock copolymer, **12** (p:m=100:0); (c) diblock copolymer, **13** (p:m=40:100); (d) diblock copolymer, **14** (p:m=10:100).

Preparation and characterization of the 2nd PS series of polymers for control experiments

The method for the polymerization of pure monomer **5** (Scheme 8) was the same as the one employed in the polymerization of PS. This involved stirring in chlorobenzene at 125 °C for 2 hours. After three precipitations into methanol, and drying under vacuum for three days, the homopolymer was isolated as a light-yellow powder. The molecular weights of homopolymer **15** calculated from ^{1}H NMR (using the same strategy mentioned above) and obtained from GPC are given in Table 2. The molar feed ratio of **5**:**1** was 30:1, and the calculated molecular weights from both analysis were close, approximately 12,000 Da. This indicates that nearly quantitative conversion was achieved, and monomer **5** could be homopolymerized to reasonable molecular weights.

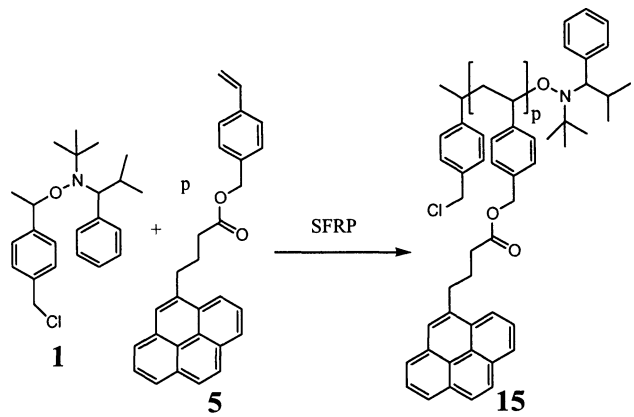

Scheme 8. Homopolymerization of monomer **5**

The same conditions as described previously were applied to synthesize random copolymers, composed of styrene and monomer **5** (Scheme 9) via SFRP.

Two different feed ratios of **5** to styrene were used: 40:100 (**16**) and 10:100 (**17**), respectively.

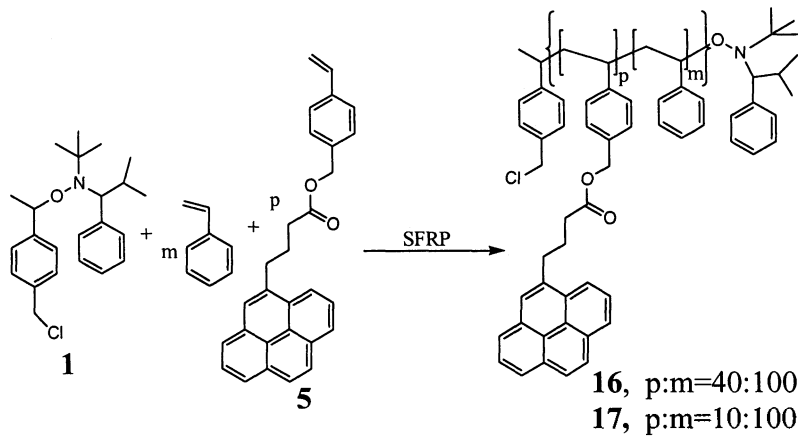

Scheme 9. Random copolymerization of styrene and monomer **5**

GPC and ^{1}H NMR were employed to characterize the final product. The molecular weights calculated from NMR and attained from GPC are listed in Table 2. Comparison of the data in Table 1 and Table 2 indicates that for compounds **16** and **17**, the actual ratios of p:m (monomer **5**:styrene) were exactly the same as the feed ratios, whereas for polymers **13** and **14**, the actual ratios of p:m were different from the feed ratios. This data suggests that the incorporation of the monomer **5** is more difficult when using the macroinitiator (**11**) than when the small-molecule initiator **1** is used. It is possible that steric hindrance plays a role in controlling monomer incorporation after initiation with a macromolecule. Although we do not have a complete understanding of this phenomenon, the pyrene-containing PS series of diblock copolymers were successfully synthesized,

and were adequate for the investigation of s-SWNTs solubilization via supramolecular interactions.

Table 2. Characteristics of the 2nd PS series of polymers

Polymers	Feed Ratio (p:m)	p (NMR[a])	m (NMR[a])	Mn		PDI
				NMR[a]	GPC[b]	GPC[b]
15	100:0	30	0	12,100	11,000	1.18
16	40:100	10	25	6,600	6,000	1.25
17	10:100	8	80	12,200	11,000	1.12

[a]Determined by ^{1}H NMR spectroscopy comparing the integration of initiator **1** signal at 4.65 ppm to the signal of the polymer at 3.3 and 6.2-7.4 ppm. [b]Determined using polystyrene standards.

3.2.2 Preparation and characterization of the PMMA series of diblock copolymers

In order to expand the scope of this project, we chose to also investigate pyrene-functionalized diblock copolymers utilizing acrylate-based monomers. ATRP was chosen for the polymerization of these acrylate monomers. Following previously developed procedures from our lab,[98] 2-bromo-2-methyl-propionyl bromide **18** was selected as the initiator and CuBr/bipyridine as the catalyst/ligand for the polymerization of MMA. The polymerization was carried out in a mixture of water and dimethylformide (DMF) at room temperature for two hours.

Scheme 10 illustrates the synthesis of PMMA **19**. Since H_2O is used in this reaction, the 2-bromo-2-methyl-propionyl bromide **18** is hydrolyzed to form 2-bromo-2-methyl propionic acid, resulting in the acid functionalized PMMA **19**. The polymer samples were then dissolved in a small amount of CH_2Cl_2, and filtered through basic Al_2O_3 on a thin layer of celite (to effectively remove the copper salts). The polymers were then isolated by precipitation into cold methanol, which was repeated three times.

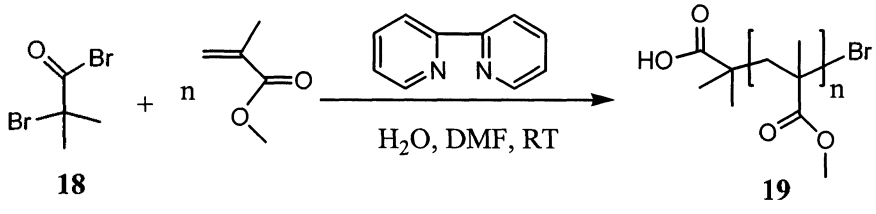

18 **19**

Scheme 10. Homopolymerization of MMA by ATRP

Monitoring of the polymerization by GPC showed relatively nice control over the molecular weight and polydispersity (Figure 19). All copper salts were effectively removed before GPC analysis, as could be determined from the disappearance of the green colour after filtration. ^{1}H NMR and ^{13}C NMR were also utilized to characterize the final product. Using the methods outlined for the PS series of polymers (section 3.2.1), the molecular weight of PMMA **19** was calculated from ^{1}H NMR and obtained from GPC (Table3).

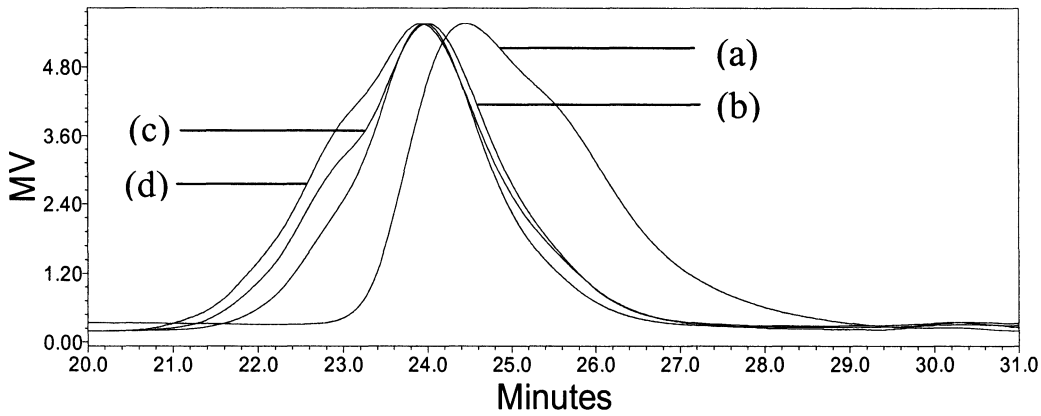

Figure 19. Comparison of GPC traces for (a) the starting polymer, **19**; (b) Poly[MMA-*b*-(acrylate-pyrene)] diblock copolymer, **20** (p:m=100:0); (c) Poly{MMA-*b*-[(acrylate-pyrene)-*r*-MMA]} diblock copolymer, **21** (p:m=40:100); (d) Poly{MMA-*b*-[(acrylate-pyrene)-*r*-MMA]} diblock copolymer, **22** (p:m=10:100).

Table 3. Characteristics of the PMMA series of polymers

Polymers	Feed Ratio (p:m)	n (NMR[a])	p (NMR[a])	m (NMR[a])	Mn NMR[a]	Mn GPC[b]	PDI GPC[b]
19	0	90	0	0	9,000	10,000	1.39
20	100:0	90	6	0	11,000	16,500	1.39
21	40:100	90	5	55	16,000	15,500	1.36
22	10:100	90	3	75	17,500	15,500	1.26

[a]Determined by ^{1}H NMR spectroscopy comparing the integration of initiator **18** signal at 1.13 ppm to the signal of the polymer at 3.60 and 7.6-8.4 ppm. [b]Determined using polystyrene standards.

Preparation and characterization of the PMMA series of diblock copolymers

The preparation of the PMMA series of diblock copolymers was accomplished by the polymerization of MMA and acrylate-pyrene monomer **8** using polymer **19** as the macroinitiator (Scheme 11). Three different feed ratios of **8**:MMA were applied in the second block, including 100:0 (**20**), 40:100 (**21**), and 10:100 (**22**), respectively (the same as the PS series of diblock copolymers). Polymer **20** was obtained in DMF at 50°C. Polymer **21** and **22** were obtained in a mixture of H_2O and DMF at room temperature. For all three reactions, the polymerization time applied was around 12 hours and the work-up procedure was the same as described for the first block, polymer **19**.

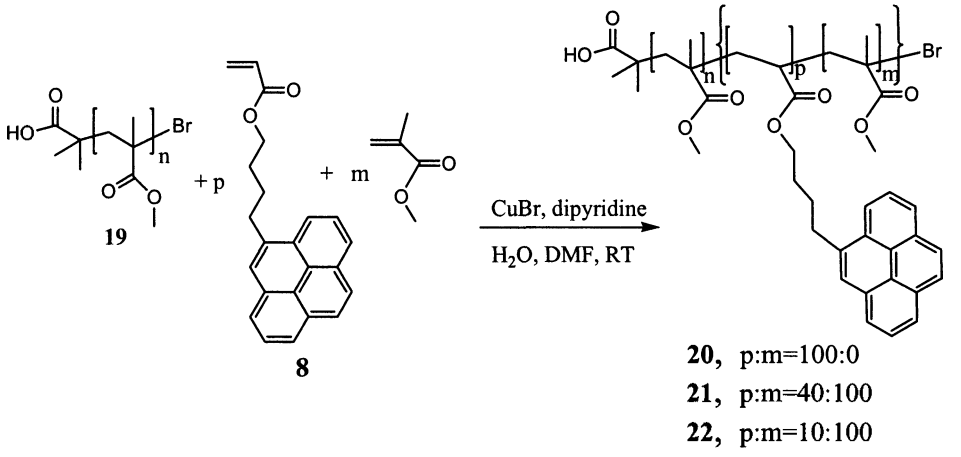

Scheme 11. Preparation of the PMMA series of diblock copolymers

The formation of the three diblock copolymers was determined by GPC, ^{1}H NMR and ^{13}C NMR measurements. The GPC traces of the resulting polymers, depicted in Figure 19, clearly show that the molecular weights of all three diblock

copolymers increased from that of the macroinitiator. In addition, all of the isolated polymers had a relatively narrow polydispersity, below 1.40.

In order to confirm that the chain-extended polymers had incorporated the monomer **8**, it was possible to utilize a fluorescence detector during the GPC measurement. The chromatograms recorded using the fluorescence detector are presented in Figure 20, and indicate that all three diblock copolymers are fluorescent, while the first block, PMMA, has no fluorescence. This experiment confirms that monomer **8** has been successfully incorporated into the second block.

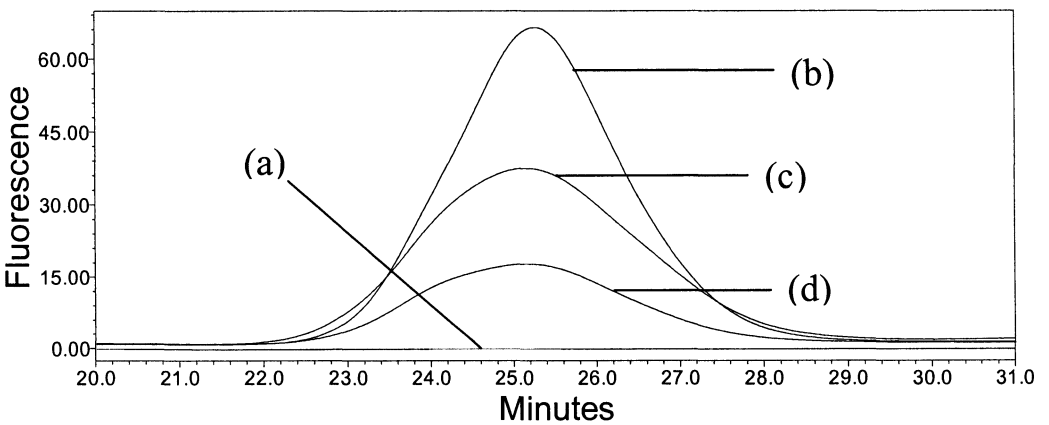

Figure 20. Comparison of fluorescence curves for (a) the starting polymer, **19**; (b) diblock copolymer, **20** (p:m=100:0); (c) diblock copolymer, **21** (p:m=40:100); (d) diblock copolymer, **22** (p:m=10:100).

The compositions of the acrylate-based series of polymers calculated from both GPC and NMR data are listed in Table 3. For polymers **19**, **21** and **22**, the molecular weights obtained from GPC and NMR data are in close agreement, while the data for polymer **20**, where the second block contains only monomer **8**,

has a much higher discrepancy. It may be possible that the rigidity of this second block, impacted by the π-stacking of pyrene groups, may cause the apparent hydrodynamic volume of the polymer to be disproportionately large, resulting in the observed overestimation of the polymer molecular weight by size-exclusion chromatography.

3.2.3 Preparation and characterization of the P(*t*-BA) series of diblock copolymers

As a further extension of acrylate-based monomers, we decided to explore the use of *t*-butyl acrylate to prepare a third series of polymers. This monomer was chosen based on the high organic-solubility of poly(*t*-BA), as well as the possibility to remove the *t*-butyl groups in order to prepare poly(acrylic acid). The latter polymer is soluble in aqueous solvents, allowing us to switch the solubility of the polymer-nanotube materials that we were interested in preparing. ATRP was employed to synthesize the P(*t*-BA) series of diblock copolymers. Ethyl 2-bromopropionate (2-EBP) **23**, was selected as the initiator and CuBr/*N,N,N',N',N''*-pentamethyldiethylenetriamine (PMDETA) as the catalyst/ligand system for the polymerization of *t*-BA. The polymerization was carried out in DMF at 55 °C for two hours.

Scheme 12 illustrates the synthesis of the macroinitiator, P(*t*-BA), **24**. The polymerization occurred smoothly at 55°C in bulk yielding a relatively well-defined homopolymer with a polydispersity around 1.30 (Table 4). The work up

procedure was the same as described for polymer **19**, except that P(*t*-BA) was purified by precipitation into a mixture of methanol and water (7:3). Using the same method as mentioned in 3.2.1, the molecular weight could be obtained from both ^{1}H NMR and GPC, which is listed in Table 4.

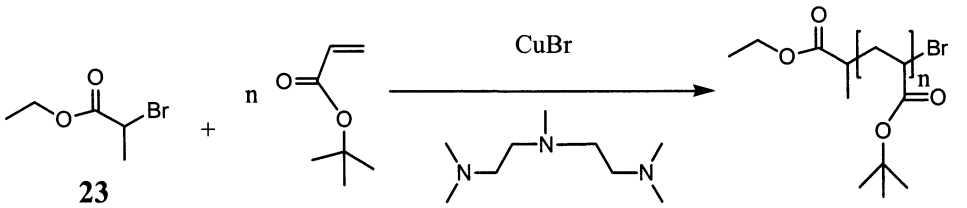

23 **24**

Scheme 12. Homopolymerization of P(*t*-BA)

Table 4. Characteristics of the P(*t*-BA) series of polymers

Polymers	Feed Ratio (p:m)	n (NMR[a])	p (NMR[a])	m (NMR[a])	Mn NMR[a]	Mn GPC[b]	PDI GPC[b]
24	0	78	0	0	10,000	13,900	1.29
25	100:0	78	9	0	13,000	19,400	1.40
26	40:100	78	5	28	15,000	22,500	1.33
27	10:100	78	3	44	16,500	22,400	1.35

[a]Determined by ^{1}H NMR spectroscopy comparing the integration of initiator **23** signal at 4.16 ppm to the signal of the polymer at 2.20 and 7.6-8.4 ppm. [b]Determined using polystyrene standards.

Preparation and characterization of the P(*t*-BA) series of diblock copolymers

The preparation of the P(*t*-BA) series of diblock copolymers was accomplished by the polymerization of *t*-BA and monomer **8** using polymer **24** as the macroinitiator in DMF at 55°C. Scheme 13 depicts the formation of the desired polymer, P(*t*-BA) series. The feed ratios of monomer **8** to *t*-BA of the second block were 100:0, 40:100, and 10:100, respectively, which were the same as the PS and PMMA series. The diblock copolymers were purified by flash chromatography on silica gel, eluting with pure CH_2Cl_2. This resulted in the isolation of pure polymers in the form of a pale yellow solid.

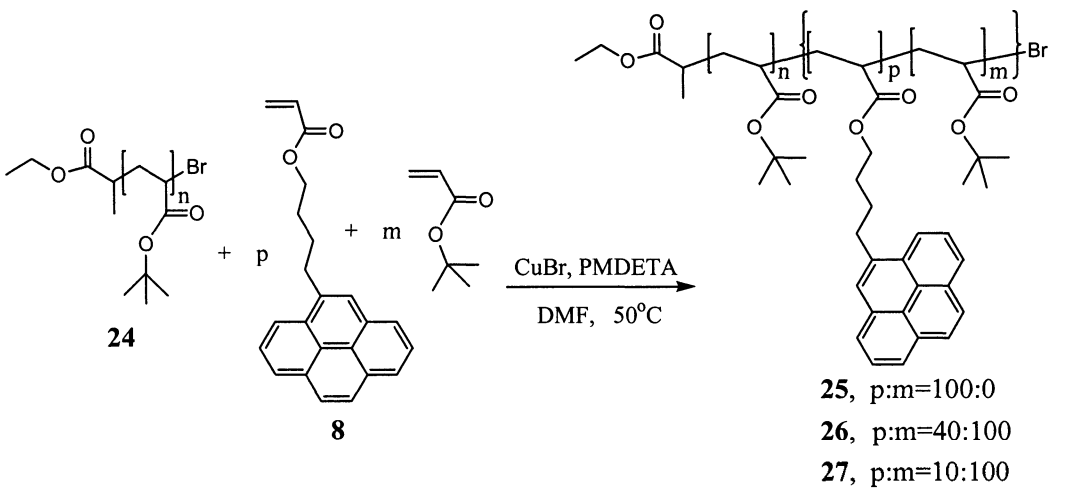

24

8

25, p:m=100:0
26, p:m=40:100
27, p:m=10:100

Scheme 13. Preparation of the P(*t*-BA) series of diblock copolymers

Figure 21 exhibits the chromatograms of the P(*t*-BA) series of polymers recorded using the fluorescence detector. It clearly shows that monomer **8** has been successfully incorporated into the second block. The compositions of the polymers obtained from both ^1H NMR and GPC are listed in Table 4. The

molecular weight of each polymer calculated from NMR is much higher than the molecular weight obtained from GPC. Here, the discrepancy is most likely due to the GPC calibration curve, which was created using polystyrene standards. Since this series of polymers has chemical and physical characteristics that are very different from polystyrene, it cannot be expected that the absolute molecular weight would be correctly determined by GPC.

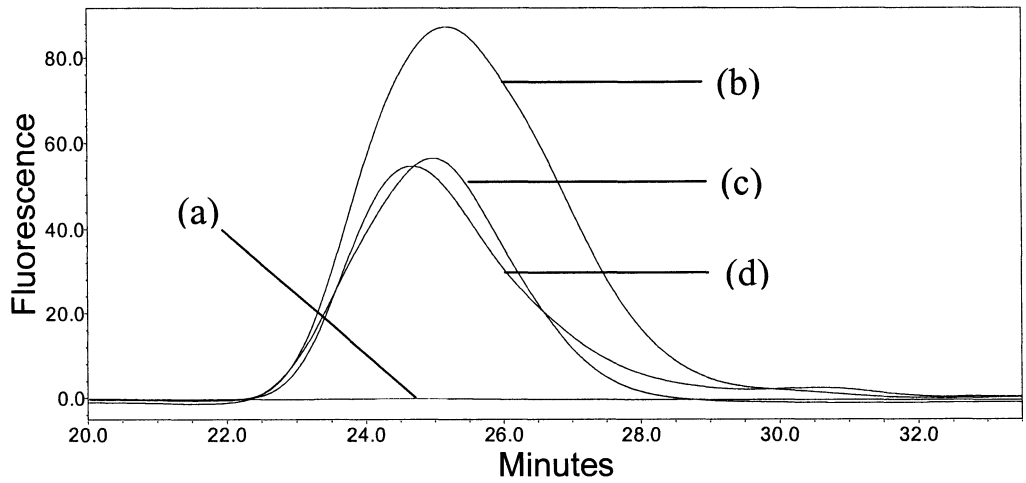

Figure 21. Comparison of fluorescence curves for (a) the starting polymer, **24**; (b) Poly[(*t*-BA)-*b*-(acrylate-pyrene)] diblock copolymer, **25** (p:m=100:0); (c) Poly{(*t*-BA)-*b*-[(acrylate-pyrene)-*r*-(*t*-BA)]} diblock copolymer, **26** (p:m=40:100); (d) Poly{(*t*-BA)-*b*-[(acrylate-pyrene)-*r*-(*t*-BA)]} diblock copolymer, **27** (p:m=10:100).

3.2.6 Synthesis and characterization of the PAA series of diblock copolymers

Scheme 14 illustrates the deprotection of the P(*t*-BA) series of diblock copolymers to form the PAA series of polymers. Selective deprotection of the

tert-butyl groups in the presence of pyrene butyl esters was achieved by treatment with trifluoracetic acid (TFA) in anhydrous CH_2Cl_2 at room temperature, under nitrogen, for 12 hours.

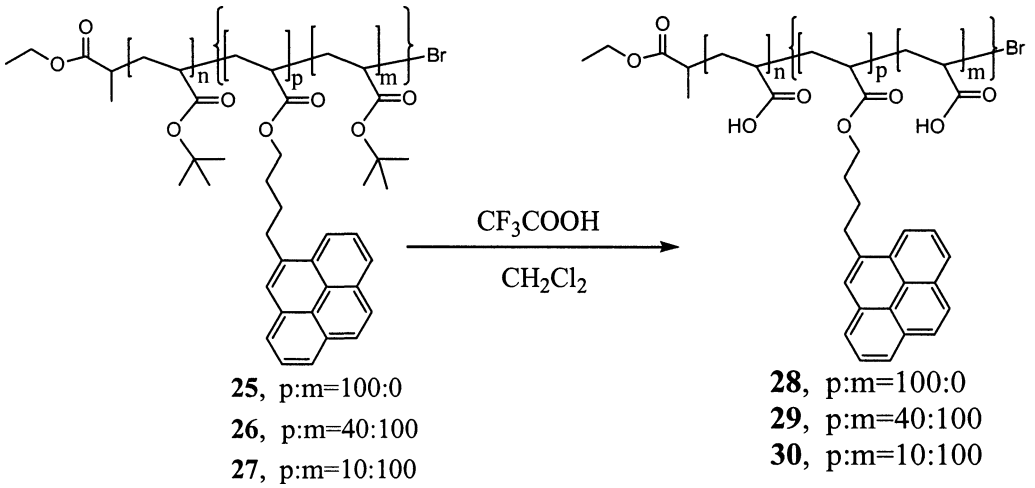

25, p:m=100:0
26, p:m=40:100
27, p:m=10:100

28, p:m=100:0
29, p:m=40:100
30, p:m=10:100

Scheme 14. Synthesis of the PAA series of diblock copolymers

The reaction was monitored by ^1H NMR. Figure 22 displays the ^1H NMR spectra of the converted product (b, polymer **29**) in D_2O and the starting material (a, polymer **26**) in $CDCl_3$. During the deprotection reaction, the signal at 1.42 ppm, resulting from the *tert*-butyl protons, decreased in intensity and finally disappeared. It was therefore possible to monitor the conversion of the *t*-BA units into the acrylic acid groups on the polymer. It should be noted that the ^1H NMR spectrum of product **29** was measured in D_2O, as it is insoluble in $CDCl_3$. It is believed that the polymer forms micelles in D_2O, where the hydrophobic pyrene units form a dense core that is surrounded by the hydrophilic PAA chains. This

micellization likely results in decreased mobility of the pyrene groups, decreasing the intensity of the proton signals that are observable from the pyrenes.

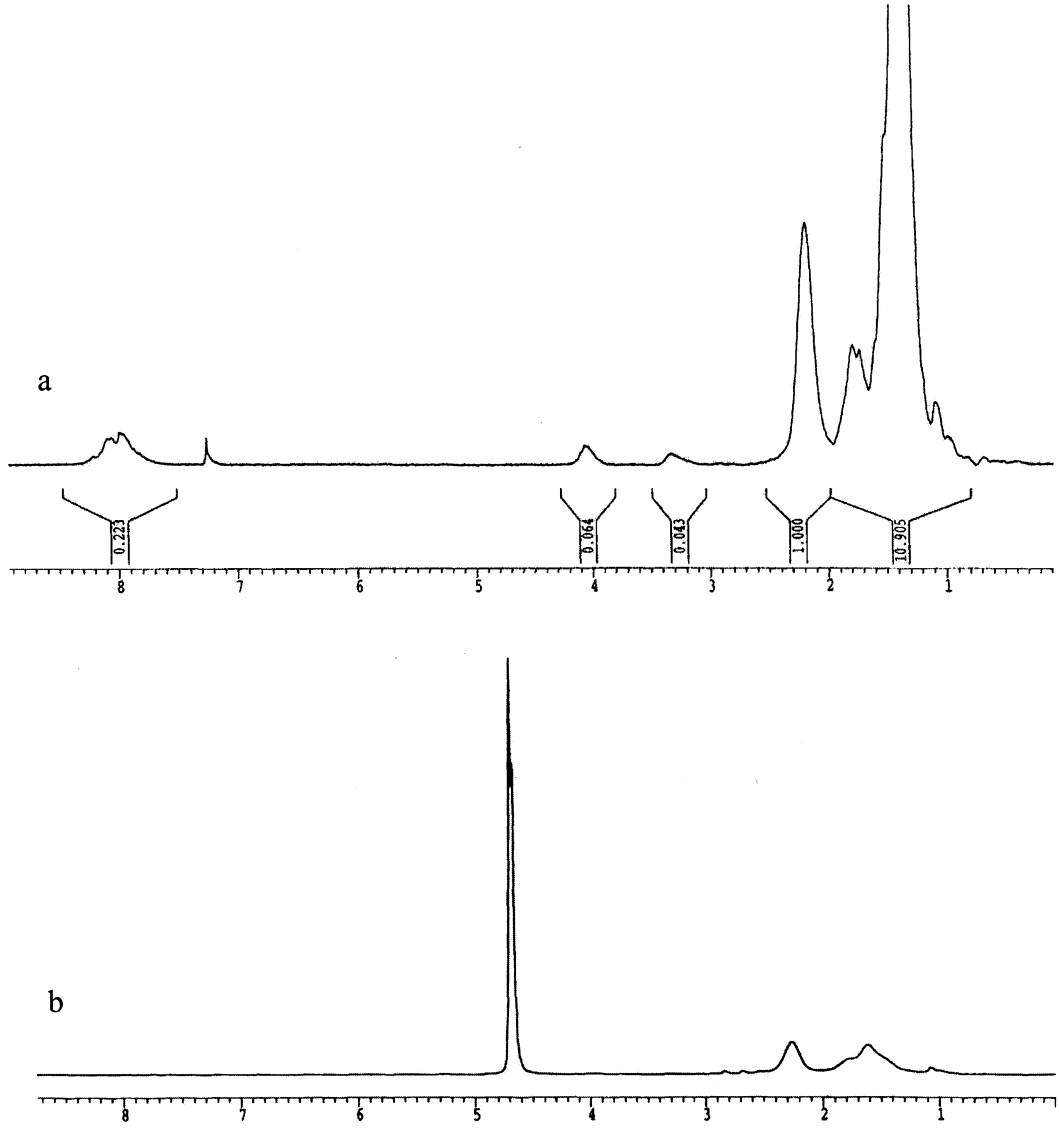

Figure 22. ^{1}H NMR spectra of (a) **26** in $CDCl_3$ and its conversion product (b) **29** in D_2O.

Figure 23 depicts the FT-IR spectra of polymer **26** (a) and that of polymer **29** (b), which is produced by the treatment of **26** with CF_3COOH. The carbonyl

stretch of 1728 cm^{-1}, as well as the C-H stretch at 2978 cm^{-1} (Figure 23, a), is both characteristic of polymer **26**. Upon conversion of **26** to **29**, the IR spectrum exhibits the expected broad absorption brand entered at ca. 3200 cm^{-1}, which is consistent with the conversion of the *t*-butyl esters in **26** to the carboxylic acids in **29**.

a.

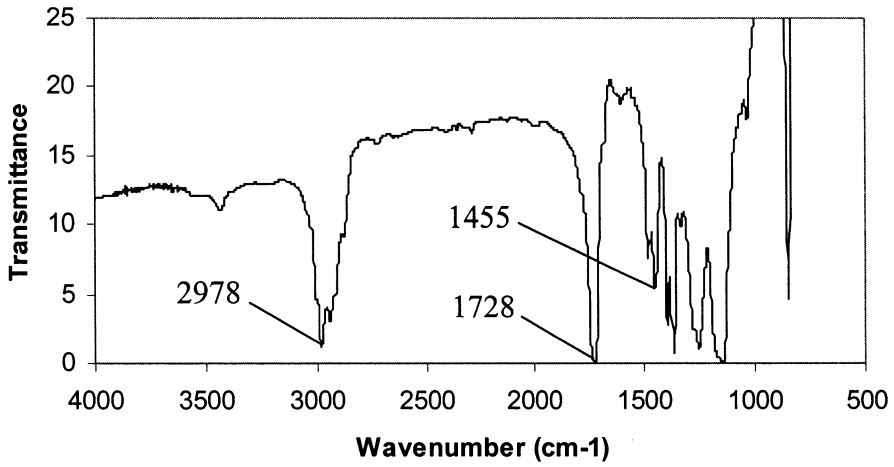

b.

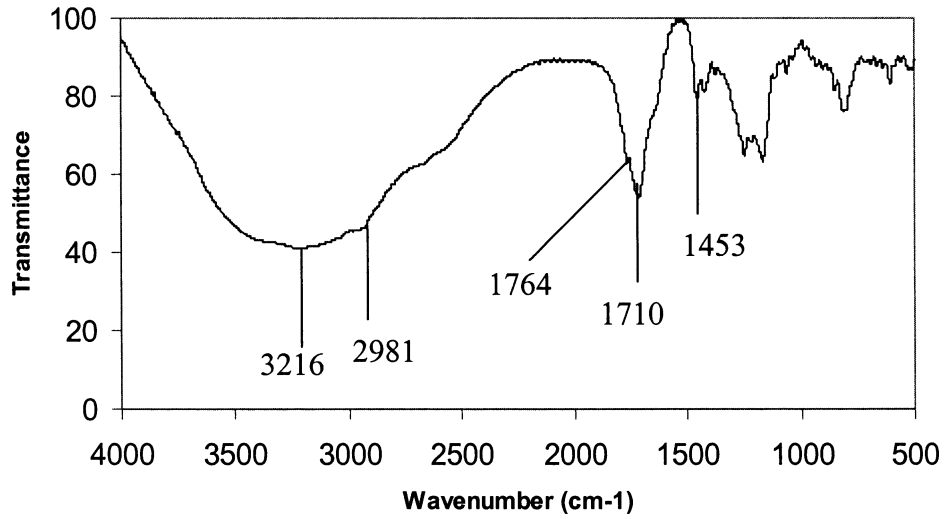

Figure 23. FT-IR spectra of (a) polymer **26** and its conversion product (b) polymer **29**.

3.3 Supramolecular functionalization of s-SWNTs with the pyrene containing diblock copolymers

Of particular interest to this work is to solubilize s-SWNTs by supramolecular functionalization with each of the synthesized pyrene-containing diblock copolymers. Shortened nanotubes were obtained by sonication in a mixture of H_2SO_4 and HNO_3, resulting in s-SWNTs process, with a length of about 350 nm.[98] The solubility was tested by mixing 10 mg of the polymer and 1 mg of s-SWNTs in 10 mL of THF (or H_2O). The mixture was sonicated for half an hour at room temperature, and allowed to stand from two weeks to more than six months. The results of supramolecular functionalization of s-SWNTs with the pyrene-containing diblock copolymers were divided into sections according to the different types of diblock copolymers.

3.3.1 Control experiments

Two series of control experiments were incorporated into our investigation to confirm that the pyrene-containing diblock copolymers are more efficient at solubilizing s-SWNTs than control polymer structures that do not contain pyrene or do not contain two different blocks. Pure PS, PMMA, P(*t*-BA), and PAA were chosen for mixing with s-SWNTs in the 1st set of control experiments. Figure 24 displays the vials containing 1.0 mg of s-SWNTs along with 10.0 mg each of PS (a), PMMA (b), and P(*t*-BA) (c) in THF. In addition, control experiments for the

aqueous soluble polymers including solutions of PAA (d), and pure nanotubes (e) in H_2O. All of the control solutions in THF remained colourless, which is consistent with pristine SWNTs being insoluble in common organic solvents. However, upon sonication of the control mixtures in H_2O, a small amount of the s-SWNTs was observed to dissolve, as evidenced by the dark colour of the solutions. Since both the solution in the presence and absence of PAA had the same degree of colour change, it can be concluded that the shortened SWNTs have the same inherent H_2O solubility, and it is not a result of interactions between the dissolved PAA with the SWNTs.

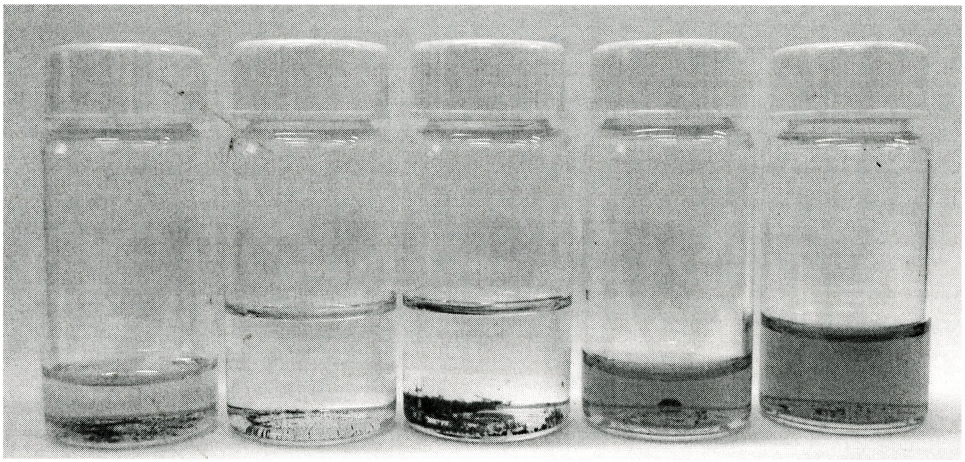

a b c d e

Figure 24. Photograph of the 1st set of control experiments: 1.0 mg of s-SWNTs added to solution of (a) PS, (b) PMMA and (c) P(*t*-BA) in THF; (d) PAA and (e) only s-SWNTs in H_2O.

Figure 25 depicts the results of another set of control experiments including the mixture of 1.0 mg of s-SWNTs in THF with 10.0 mg each of the following

pyrene-containing molecules: styrene-pyrene monomer **5** (f); homopolymer poly(styrene-pyrene) **15** (g); random copolymer poly[styrene-*r*-(styrene-pyrene)] (p:m=40:100) **16** (h); and random copolymer poly[styrene-*r*-(styrene-pyrene)] (p:m=10:100) **17** (i). Here all four solutions became slightly coloured. This slight increase in solubility is likely due to π-stacking interactions between the pyrene-functionalized molecules and the nanotube surface.

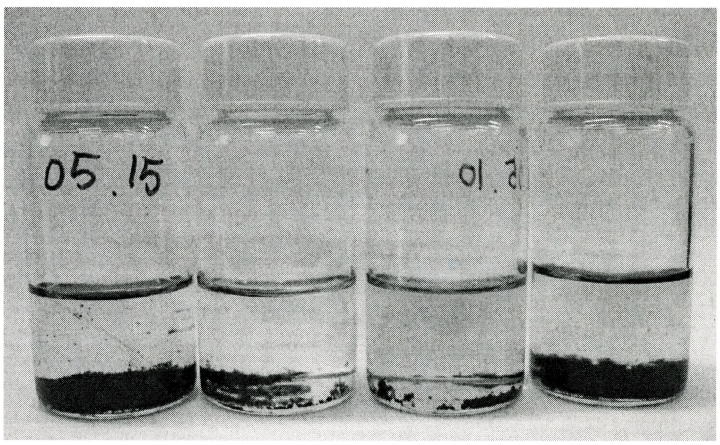

f g h i

Figure 25. Photograph of the 2nd set of control experiments: (f) monomer **5**; (g) homopolymer **15** (feed ratio of monomer **5** to styrene was 100:0); (h) random copolymer **16** (feed ratio of **5** to styrene was 40:100); and (i) random copolymer **17** (feed ratio of **5** to styrene was 10:100) mixed with 1.0 mg of s-SWNTs in THF.

In order to determine the exact nanotube concentration in these solutions, it is possible to use UV-Vis spectroscopy. It has been shown that the nanotube concentration can be determined from the absorbance at 500 nm, using the nanotube extinction coefficient ε=28.6 cm^2/mg.[97] Table 5 lists the results of the

eight control experiments, showing that the concentration of all solubilized s-SWNTs is less than 10 mg/L.

Table 5. Control experiments for room temperature solubility of s-SWNTs

Molecules		Vial	Feed Ratio of **5** to styrene	A (UV-absorption at 500 nm)	Solvent	C mg/L
PS		a	_	0.04355	THF	1.5
PMMA		b	_	0.01828	THF	0.6
P(t-BA)		c	_	0.05541	THF	1.9
PAA		d	_	0.2470	H_2O	8.7
_		e	_	0.2459	H_2O	8.6
Pyrene Monomer **5**		f	_	0.07431	THF	2.6
Homo Pyrene Polymer **15**		g	100:0	0.05804	THF	2
Random Block Copolymer	**16**	h	40:100	0.1173	THF	4.1
	17	i	10:100	0.1813	THF	6.3

3.3.2 Supramolecular functionalization of s-SWNTs with the PS series of diblock copolymers

A Photograph of the solutions resulting from mixtures of s-SWNTs with one of the three synthesized PS series of diblock copolymers in THF is shown in

Figure 26. Solutions (b) and (c), containing polymer **13** and **14** (feed ratios of monomer **5** to styrene of the 2nd block were 40:100 and 10:100, respectively) are darker than (a), which contains polymer **12** (feed ratio of monomer **5** to styrene of the 2nd block was 100:0). Additionally, we observed that not all of the s-SWNTs dissolved in the polymer mixture. This may be due to a solubility limit for the SWNTs, or due to the heterogeneous nature of the SWNTs, where structures that are extremely long or clumped into very large bundles are less soluble than shorter, less bundled SWNTs.

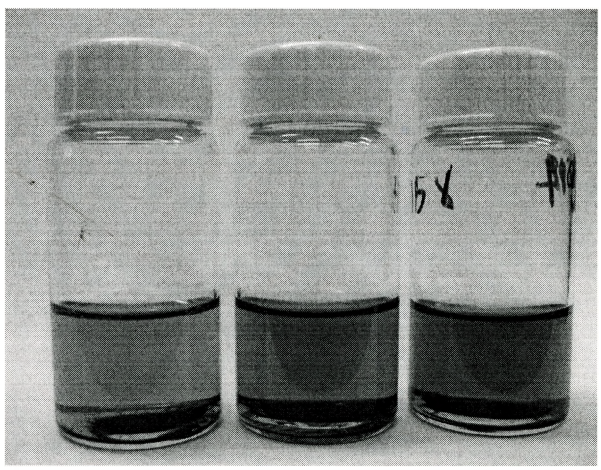

a b c

Figure 26. Supramolecular functionalization of s-SWNTs with each of the PS series of diblock copolymers in THF: (a) **12** (feed ratio of monomer **5** to styrene of the 2nd block was 100:0); (b) **13** (feed ratio of **5** to styrene of the 2nd block was 40:100); (c) **14** (feed ratio of **5** to styrene of the 2nd block was 10:100).

Interestingly, a 5-fold increase in the polymer concentration did not result in an increase in the amount of dissolved SWNTs. This indicates that the latter explanation, where SWNT solubility is limited by sample heterogeneity, is

mostly likely. Further experiments will have to be performed to fully understand the exact reasons for our observations.

Quantitative information about the solubility of s-SWNTs was gathered by UV-Vis absorption spectroscopy, as mentioned in section 3.3.1. The concentration of solubilized s-SWNTs in THF is listed in Table 6, and the UV-vis absorption data is consistent with the dark colour (the darker the colour, the more s-SWNTs dissolved). It appears that the polymers with a lower degree of pyrene-functionalization provided better solubilization of s-SWNTs. The explanation for this observation stems from the fact that pyrene molecules have a strong tendency to π-stack with one another. It is likely that in polymer **12**, where the second block is entirely composed of pyrene-functionalized monomers, the pyrene units are intra-molecularly π-stacking. In order for these polymers to form interactions with SWNTs, the intra-molecular π-stacking must be disrupted, a process that is not energetically favourable. Conversely, in polymer **14**, where the second block contains only 10% of the pyrene-functionalized monomer, the probability that two pyrenes are close enough to one another to form excimers is much lower, leaving the structures to interact with the nanotube surface. Therefore, it is predicted that lower pyrene concentrations within the second block should result in better SWNT solubility, up until a certain limit at which further decreasing the pyrene concentration will result in diminished solubility due to a decrease in the number of sites for interaction.

Table 6. Room temperature solubility of supramolecular functionalized s-SWNTs with each of the PS series of diblock copolymers in THF

Vials	Polymers	A (UV, 500 nm)	C (mg/L)
a	**12**	0.3175	11
b	**13**	0.4494	16
c	**14**	0.7847	27

Microscopy analysis

The most direct evidence for the presence of carbon nanotubes in solution can be determined from microscopy analysis, such as Atomic Force Microscopy (AFM) and Transmission Electron Microscopy (TEM) of the solutions. The supramolecularly functionalized s-SWNTs in solution were deposited directly onto a fresh mica surface for AFM and TEM analysis.

Figure 27 shows s-SWNT/polymer conjugates observed by AFM. From this figure, it is possible to discern nanotube bundles that are embedded within a film of polymers, which covers the entire surface. This is consistent with expectations since there is a large excess of polymer within the solutions.

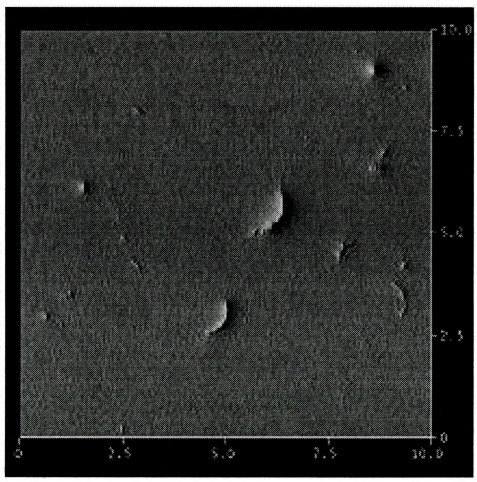

Figure 27. AFM image of dissolved **14**/ SWNT composites.

TEM analysis of the functionalized carbon nanotubes is especially useful in providing both an overview at low magnification and a detailed examination at high-resolution. Bundles of s-SWNTs can be observed stretching out from the polymer matrix under high resolution TEM (Figure 28, a). At low magnification (Figure 28, b), it is possible to see polymer films that contain nanotube bundles within them. In particular, one enlarged section displays only 1 or 2 single nanotubes, spanning the gap between two areas of polymer. The presence of these small bundles and individual tubes may indicate that the pyrene-functionalized polymers are actually breaking up the large bundles into smaller ones, thus rendering s-SWNTs soluble in THF.

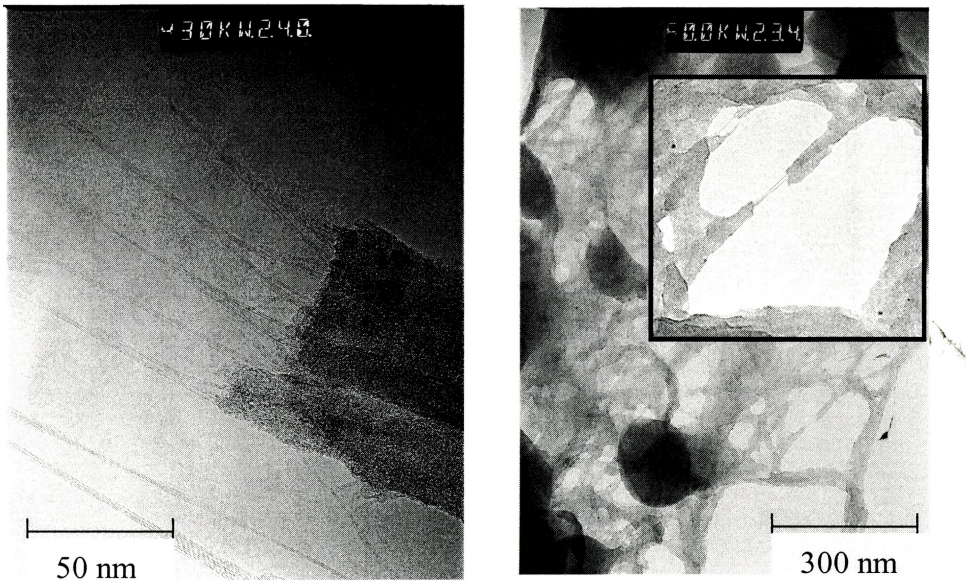

(a) High magnification TEM (b) Low magnification TEM

Figure 28. TEM images of dissolved **14**/SWNT composites.

3.3.3 Supramolecular functionalization of s-SWNTs with the PMMA series of diblock copolymers

A photograph of s-SWNTs mixed with one of the three synthesized PMMA series diblock copolymers in THF is shown in Figure 29. Vials (b) and (c), containing **21** and **22** (feed ratios of monomer **8** to MMA of the 2nd block were 40:100 and 10:100, respectively) are much darker than vial (a), which contains **20** (feed ratio of **8** to MMA of the 2nd block was 100:0). The trend of the colour change is the same as the one observed in Figure 26 for the PS series of polymers. UV-Vis absorption spectroscopy was also used to determine the solubility of these polymer-SWNT conjugates, and the concentration of the

solubilized SWNTs in THF is listed in Table 7. The UV-vis absorption data is consistent with the dark colour, showing again that the least pyrene-containing polymer improves the solubility of s-SWNTs most. Additionally, if the feed ratio of the second block is the same, each diblock copolymer in the PMMA series gives better solubility than the corresponding diblock copolymer in the PS series. Again, TEM was utilized to image the solubilized Poly{MMA-*b*-[MMA-*r*-(acrylate-pyrene)]}/SWNT conjugates. Similar results to the ones previously showed (Figure 28) were obtained, where small ropes of SWNTs were observed.

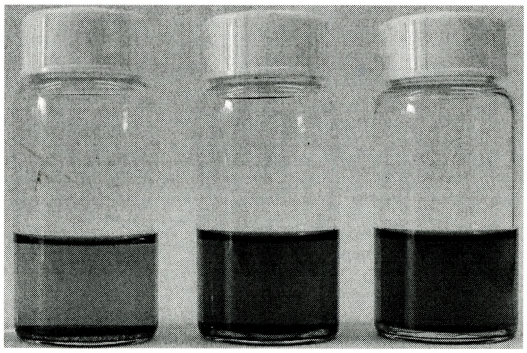

a b c

Figure 29. Supramolecular functionalization of s-SWNTs with each of the PMMA series of diblock copolymers in THF: (a) **20** (feed ratio of monomer **8** to MMA of the 2nd block was 100:0); (b) **21** (feed ratio of **8** to MMA of the 2nd block was 40:100); (c) **22** (feed ratio of **8** to MMA of the 2nd block was 10:100).

Table 7. Room temperature solubility of supramolecular functionalized s-SWNTs with each of the PMMA series of diblock copolymers in THF

Vials	Compound number	A (UV, 500 nm)	C (mg/L)
a	**20**	0.4638	16
b	**21**	1.0276	36
c	**22**	1.1777	41

3.3.4 Supramolecular functionalization of s-SWNTs with the P(*t*-BA) series of diblock copolymers

Figure 30 shows the results of s-SWNTs mixed with one of the three synthesized P(*t*-BA) diblock copolymers in THF. Vials (b) and (c), containing polymer **26** and **27** (feed ratios of monomer **8** to *t*-BA of the 2nd block were 40:100 and 10:100, respectively) are much darker than Vial (a), which contains polymer **25** (feed ratio of **8** to *t*-BA of the 2nd block was 100:0). Again, the same results were obtained as those shown in Figure 26 and in Figure 29, where the darkest vial contains the polymer having the lowest pyrene concentration. Table 8 lists the concentration of solubilized s-SWNTs in THF calculated from UV spectroscopy. The UV data is consistent with the dark colour. However, this time, each polymer of the P(*t*-BA) series is less effective in solubilizing s-SWNTs than the corresponding polymers (the same feed ratios of p:m in the 2nd block) of the PS series and the PMMA series.

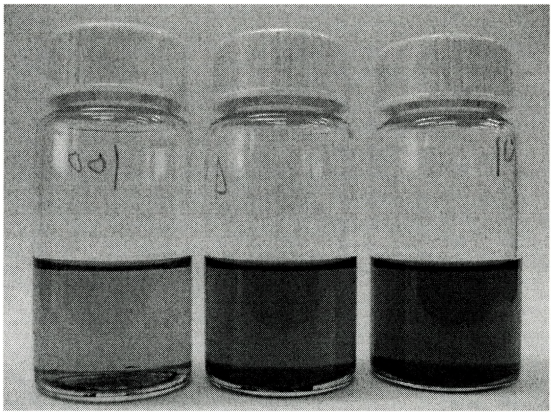

a b c

Figure 30. Supramolecular functionalization of s-SWNTs with each of the P(*t*-BA) series of diblock copolymers in THF: (a) polymer **25** (feed ratio of monomer **8** to *t*-BA in the 2nd block was 100:0); (b) polymer **26** (feed ratio of **8** to *t*-BA in the 2nd block was 40:100); (c) polymer **27** (feed ratio of **8** to *t*-BA in the 2nd block was 10:100).

Table 8. Room temperature solubility of supramolecular functionalized s-SWNTs with each of the P(*t*-BA) series of diblock copolymers in THF

Vials	Compound number	A (UV, 500 nm)	C (mg/L)
a	**25**	0.1983	7
b	**26**	0.3510	12
c	**27**	0.4638	16

3.3.5 Supramolecular functionalization of s-SWNTs with the PAA series of diblock copolymers

Figure 31 shows the results of s-SWNTs mixed with each of the three synthesized PAA series of diblock copolymers in H_2O. Vials (b) and (c), containing polymer **29** and **30** (converted from polymer **26** and **27**, respectively) are much darker than vial (a), which contains polymer **28** (converted from polymer **25**). Vial (c) has the darkest solution, and the trend is consistent with Figure 26, Figure 29 and Figure 30. The concentration of solubilized SWNTs in aqueous solutions of each of these polymers was calculated from UV spectroscopy, and is listed in Table 9. The UV data is consistent with the dark colour of each vial, and again shows that the polymer having the lowest pyrene concentration provides the best solubilization of s-SWNTs. It is worth mentioning that the PAA series imparted the highest solubility to the s-SWNTs out of the polymer series that we investigated.

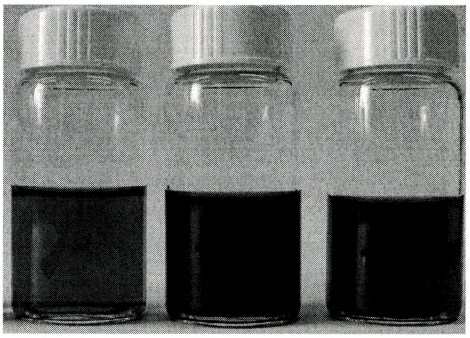

a b c

Figure 31. Supramolecular functionalization of s-SWNTs with each of the PAA series of diblock copolymers in H_2O: (a) polymer **28**, converted from polymer **25**; (b) polymer **29,** converted from polymer **26**; (c) polymer **30**, converted from polymer **27**.

Table 9. Room temperature solubility of supramolecular functionalized s-SWNTs with each of the PAA series of diblock copolymers in H_2O

Vials	Compound number	A (UV-Vis, 500 nm)	C (mg/L)
a	**28**	0.4862	17
b	**29**	1.4040	49
c	**30**	2.0420	71

Chapter 4 Conclusions

We have developed a simple methodology for solubilization of s-SWNTs via supramolecular functionalization with pyrene-containing diblock copolymers. Four series of the designed diblock copolymers were successfully synthesized, where the first block contained pure PS, PMMA, P(*t*-BA), or PAA, and the second block was composed of synthetic pyrene-functionalized monomers mixed with different amounts of monomers that match the composition of the first block. SFRP and ATRP were employed in our investigation. The selective cleavage of *tert*-butyl groups from the P(*t*-BA) series afforded a water-soluble polymer, which broadens the solubility properties from organic solvents to aqueous media.

We have shown that all of these four series of diblock copolymers form stable solutions with s-SWNTs in THF or H_2O, depending on the solubility of the first block. Comparing to the eight control experiments, we could draw the conclusion that the first block in our diblock copolymers was utilised to increase the solubility, and the second block containing the pyrene moiety was used to strongly interact with s-SWNTs, together forming a soluble polymer-SWNT conjugate.

The whole process requires an important condition, sonication of the mixture in the solvent to break up the SWNTs bundles and maximize cooperative interactions between nanotubes and polymers. Additionally, we discovered from TEM studies that the polymers were able to wrap around individual carbon

nanotubes. It might therefore be possible to isolate single tubes through our supramolecular functionalization.

For all of four series of diblock copolymers, the individual polymers from each series having the lowest pyrene concentration within the second block resulted in the best solubility of s-SWNTs. Among them, polymer **30**, whose first block was PAA, offered the highest ability of solubilizing s-SWNTs, resulting in a nanotube concentration of approximately 71 mg/L in H_2O.

Chapter 5 Experimental

General

Styrene (Aldrich; 99%), MMA (Aldrich; 99%), *t*-BA (Aldrich; 99%) were purified by column chromatography on basic alumina gel and stored in the refrigerator. Copper (I) bromide (Aldrich; 99%) was stored under argon at room temperature. Bipyridine (99%), N,N,N',N',N''-pentamethylethylenetriamine (PMDETA, 99%), ethyl-2-bromo-propoionate (2-EBP, 99%), 2-bromo-2-methyl-propionyl bromide (98%), 1-Pyrenebutanol (99%), 1-pyrenebutyric acid (97%), 4-vinylbenzyl chloride (90%), acryloyl chloride (96%), and 18-crown-6 (99%) were purchased from Aldrich and used without further purification. The nitroxide initiator, 2,2,5,5-tetramethyl-3-(1-phenylethoxy)-4-chloromethylphenyl-3-azahexane, compound **1** and the free nitroxide radical, 2,2,5,5-tetramethyl-4-phenyl-3-azahexane-3-nitroxide, compound **2** were prepared following the procedure reported by Hawker and coworkers.[94] SWNTs (Carbon Nanotechnologies Inc.) were purified and shortened by methods previously reported by our group.[98] Other reagents and solvents were purchased from Aldrich and used as received.

Analytical thin-layer chromatography (TLC) was performed on commercial Merck plates coated with silica gel GF254 (0.25 mm thick). Silica gel for flash chromatography was Merck Kieselgel 60 (230-400 mesh).

Nuclear magnetic resonance (NMR) spectroscopy was performed on a Bruker 200 or 500 MHz NMR spectrometer using deuterated chloroform ($CDCl_3$) or deuterium oxide (D_2O) as solvent at room temperature.

Molecular weights and molecular weight distributions of synthesized macroinitiators and copolymers were estimated by gel permeation chromatography (GPC) using a Waters 2695 Separations Module connected to a Waters 2414 Refractive Index Detector, Waters 2996 Photodiode Array Detector, and Waters 2475 Multi λ Fluorescence Detector with tetrahydrofuran (THF) as the carrier solvent at a flow rate of 1.0 mL/min. Molecular weight standards used for calibration of the GPC system were narrow polydispersity polystyrene. All samples were run in THF at 35°C. The fluorescence detector was set to an emission wavelength of 450 nm, and an excitation wavelength of 350 nm.

FTIR was measured on a FTS-40 instrument. All samples were prepared as pellets using spectroscopic grade KBr in a Carver press at 15,000 psi.

Atomic force microscopy (AFM) experiments were carried out in air with a Digital Instruments NanoScope IIIa Multimode system operated with standard silicon tips in tapping mode at a scan rate of 0.5 Hz. The samples were prepared for AFM analysis by depositing a drop from sample solutions onto mica and allowing it to dry freely in air.

TEM was recorded on a Philips CM12 instrument operating at 120 keV.

The concentration of soluble polymer-SWNT conjugates was estimated from UV-Vis absorption using a Varian Cary 50 Bio UV-Visible

Spectrophotometer. All samples were measured in spectroscopic grade THF or H_2O at room temperature.

Synthesis of styrene-pyrene monomer **5**

1-Pyrenebutyric acid (3.02 g, 10.4 mmol, 1 eq.), potassium carbonate (3.34 g, 24.2 mmol, 2.3 eq.) and 18-Crown-6 (0.301 g, 1.14 mmol, 0.1 eq.) were added to 200 mL of acetone. The mixture was refluxed for 30 minutes. It became yellow and some white solid precipitated. Then, 4-vinylbenzyl chloride (2.03 g, 13.2 mmol, 1.3 eq.) was added and the mixture was refluxed for another 6 hours. The reaction mixture was filtered through celite to remove the solid. The solvent was evaporated, and then purified by column chromatography using 5:5 CH_2Cl_2/hexanes as the eluent. After drying under vacuum overnight, 4.03 g of purified product (yellow powder) was obtained (93% yield). ^{1}H NMR (500 MHz, $CDCl_3$): δ 2.24 (q, *J*=7.3, 2H), 2.52 (t, *J*=7.0, 2H), 3.39 (t, *J*=7.6, 2H), 5.15 (s, 2H), 5.28 (d, *J*=5.3, 1H,), 5.76 (d, *J*=7.8, 1H,), 6.74 (q, *J*=5.4, 1H), and 7.31-8.29 (m, 9H). ^{13}C NMR (50 MHz, $CDCl_3$): δ 28.0, 33.9, 35.1, 67.2, 115.6, 124.5, 126.0, 126.2, 127.1, 127.7, 128.0, 128.5, 128.6, 128.7, 129.8, 131.1, 132.1, 132.6, 136.8, 137.6, 138.8, and 174.5. M.S. (E. I.): m/z 404 [M^+], calcd m/z 404.

Synthesis of acrylate-pyrene monomer **8**

To a flame dried round-bottom flask (under argon atmosphere), 1-pyrenebutanol (1.50 g, 5.47 mmol, 1 eq.) and triethylamine (3.30 g, 32.6 mmol, 6 eq.) were added along with 50 mL of dry CH_2Cl_2. It was allowed to stir for 10 minutes, until the 1-pyrenebutanol dissolved. Acryloyl chloride (0.984 g, 10.9 mmol, 2 eq.) was then added drop-wise using a syringe through a septum over 10 minutes, and the mixture was allowed to react for another 2.5 hours at room temperature. The solution was clear and turned to an orange colour. The reaction mixture was poured into 200 mL of water and extracted with CH_2Cl_2, 2x200 mL. The organic layers were collected and evaporated to dryness in vacuo. The product was then purified by column chromatography using CH_2Cl_2 as the eluent, and 1.62 g (90% yield) of pure product (yellow powder, fluorescent) was obtained. ^{1}H NMR (500 MHz, $CDCl_3$): δ 1.91 (q, *J*=8.1, 4H), 2.37 (t, *J*=3.6, 2H), 4.26 (t, *J*=3.1, 2H), 5.82 (d, *J*=5.1, 1H), 6.16 (q, *J*=5.1, 1H), 6.44 (d, *J*=7.9, 1H), and 7.84-8.29 (m, 9H). ^{13}C NMR (50 MHz, $CDCl_3$): δ 27.8, 28.3, 32.7, 64.2, 123.0, 124.6, 125.6, 126.4, 127.0, 127.3, 128.4, 129.6, 130.5, 131.2, 136.0, and 166.1. M.S. (C. I.): m/z 328 [M^+], calcd m/z 328.

Polystyrene, polymer **11**

Mixtures of styrene, the nitroxide initiator **1**, free nitroxide radical **2**, acetic anhydride and chlorobenzene were added to a round-bottom flask, degassed by

bubbling with nitrogen for 30 minutes, and sealed with a rubber septum under nitrogen. The feed ratios of initiator **1**: free nitroxide **2**: acetic anhydride were approximately 1: 0.05: 0.05. In a typical experiment, a round-bottom flask equipped with a magnetic stir bar was charged with styrene (10 g, 96 mmol, 150 eq.), initiator **1** (2.4×10^{-2} g, 0.64 mmol, 1 eq.), free nitroxide **2** (7.0×10^{-3} g, 3.2×10^{-2} mmol, 0.05 eq.), acetic anhydride (3.0×10^{-3} g, 3.2×10^{-2} mmol, 0.05 eq.), chlorobenzene (10 mL), and was sealed with a rubber septum. After bubbling with nitrogen for thirty minutes, the deoxygenated solution was heated to 125°C under nitrogen in a temperature-controlled oil bath overnight. The resulting polystyrene was dissolved in 2.5 mL of CH_2Cl_2 and drop-wise precipitated into 500 mL of methanol. The polymers were further purified by reprecipitation using the same procedure. After filtering and drying under vacuum, a sample of the precipitated polymer was taken up in THF (1 mg/mL) and subjected to GPC analysis. Overall yield: 9.0 g (90%). M_n^{NMR}=13,000 g/mol, M_n^{GPC}=11,500 g/mol, M_w/M_n=1.08. ^{1}H NMR (200 MHz, $CDCl_3$): δ 1.48 (br, 2H), 1.86 (br, 1H), 4.65 (s, 2H), 6.55(br, 2H), and 7.07 (br, 2H). ^{13}C NMR (50 MHz, $CDCl_3$): δ 27.8, 40.7, 44.2, 44.3, 44.4, 44.5, 44.7, 125.7, 125.9, 127.7, 127.9, 128.2, 145.5, 145.6, 145.9, and 146.3.

Poly[styrene-*b*-(styrene-pyrene)], polymer **12**

The nitroxide terminated polymer **11** (0.80 g, 7.0×10^{-2} mmol, 1 eq.), monomer **5** (0.50 g, 1.24 mmol, 18 eq.), free nitroxide **2** (7.6×10^{-4} g, 3.5×10^{-3}

mmol, 0.05 eq.), and acetic anhydride (3.6×10^{-4} g, 3.5×10^{-3} mmol, 0.05 eq.) were dissolved in 5 mL of chlorobenzene in a 20 mL round bottom flask, degassed by bubbling with nitrogen for 30 minutes, and sealed with a rubber septum under nitrogen. The polymerization was carried out in an oil bath regulated at 125°C under nitrogen for 16 hours. The viscous reaction mixture was then diluted with 1 mL of CH_2Cl_2 and precipitated into 250 mL of methanol. The solid precipitate was then collected and dissolved in 5 mL of CH_2Cl_2 and reprecipitated into 100 mL of methanol. This precipitation procedure was repeated two more times to remove monomer **5** to obtain purified product **12**. After drying under vacuum, 0.91 g of a white powder was obtained (70% yield). M_n^{NMR} = 16,500 g/mol, M_n^{GPC}=13,000 g/mol, M_w/M_n=1.18. ^{1}H NMR (500 MHz, $CDCl_3$): δ 1.46 (br, 2H), 1.88 (br, 1H), 2.09 (br, 2H), 2.41 (br, 2H), 3.24 (br, 2H), 4.65 (s, 2H), 5.01 (br, 2H), 6.60 (br, 2H), 7.08 (br, 2H), and 7.4-8.3 (br, 9H). ^{13}C NMR (50 MHz, $CDCl_3$): δ 33.7, 39.6, 40.8, 47.3, 49.5, 50.8, 73.0, 130.2, 131.7, 132.7, 133.6, 134.7, 135.0, 136.8, 137.7, 138.3, 142.5, 152.3, and 180.1.

Poly{styrene-*b*-[(styrene-pyrene)-*r*-styrene)]}, polymer **13**

Polymer **13** was prepared using the same procedure as the one employed for the polymer **12** except that the feed ratio of monomer **5** to styrene in the second block was 40:100 (**13**) instead of 100:0 (**12**). Specifically, polymer **11** (0.80 g, 7.0×10^{-2} mmol, 1 eq.), monomer **5** (0.50 g, 1.2 mmol, 18 eq.), styrene (0.38 g, 3.7 mmol, 54 eq.), free nitroxide **2** (7.6×10^{-4} g, 3.5×10^{-3} mmol, 0.05 eq.), and acetic

anhydride (3.6×10^{-4} g, 3.5×10^{-3} mmol, 0.05 eq.) were mixed in 5 mL of chlorobenzene. After polymerization at 125°C for 16 hours, the product was purified by precipitation, as outlined for polymer **12**. Yield: 1.0 g (60%). M_n^{NMR}=16,800 g/mol, M_n^{GPC}=13,500g/mol, M_w/M_n=1.22. ^{1}H NMR (500 MHz, $CDCl_3$): δ 1.44 (br, 2H), 1.86 (br, 1H), 2.15 (br, 2H), 2.43 (br, 2H), 3.32 (br, 2H), 4.57 (s, 2H), 5.06 (br, 2H), 6.60 (br, 2H), 7.03 (br, 2H), and 7.5-8.3 (br, 9H). ^{13}C NMR (50 MHz, $CDCl_3$): δ 34.0, 39.7, 40.5, 47.3, 50.2, 73.1, 131.8, 132.7, 135.0, 142.5, 152.3, and 180.1.

Poly{styrene-*b*-[(styrene-pyrene)-*r*-styrene)]}, polymer **14**

Polymer **14** was prepared using the same procedure as the one employed for polymer **12** except that the feed ratio of monomer **5** to styrene in the second block was 10:100 (**14**) instead of 100:0 (**12**). Specifically, polymer **11** (0.80 g, 7.0×10^{-2} mmol, 1 eq.), monomer **5** (0.50 g, 1.2 mmol, 18 eq.), styrene (1.5 g, 15 mmol, 212 eq.), free nitroxide **2** (7.6×10^{-4} g, 3.5×10^{-3} mmol, 0.05 eq.), and acetic anhydride (3.6×10^{-4} g, 3.5×10^{-3} mmol, 0.05 eq.) were mixed in 5 mL of chlorobenzene. After polymerization at 125°C for 16 hours, the product was purified by precipitation, as outlined for **12**. Yield: 1.2 g (53%). M_n^{NMR}=18,500 g/mol, M_n^{GPC}=16,500 g/mol, M_w/M_n=1.18. ^{1}H NMR (500 MHz, $CDCl_3$): δ 1.47 (br, 2H), 1.85 (br, 1H), 2.19 (br, 2H), 2.45 (br, 2H), 3.38 (br, 2H), 4.58 (s, 2H), 5.05 (br, 2H), 6.60 (br, 2H), 7.07 (br, 2H), and 7.5-8.3 (br, 9H). ^{13}C NMR (50 MHz, $CDCl_3$): δ 27.8,

40.7, 44.3, 44.4, 44.5, 44.9, 126.2, 125.9, 127.7, 128.1, 128.5, 129.5, 130.1, 130.4, 145.5, 145.6, 145.9, 146.3, and 177.4.

Poly(styrene-pyrene), polymer **15**

Polymer **15** was polymerized using the same procedure as the one employed in the polymer **11** preparation, except that the feed ratio of the monomer **5** to initiator **1** was 30:1. A mixture of monomer **5** (0.20 g, 0.50 mmol, 46 eq.), initiator **1** (4.0×10^{-3} g, 1.1×10^{-2} mmol, 1 eq.), free nitroxide **2** (1.2×10^{-4} g, 5.4×10^{-4} mmol, 0.05 eq.), acetic anhydride (5.5×10^{-5} g, 5.4×10^{-4} mmol, 0.05 eq.) and 0.5 mL of chlorobenzene was heated to 125°C under nitrogen for 2 hours. After diluting the reaction mixture with 1.5 mL of CH_2Cl_2, the product was purified by precipitation, as outlined for polymer **12**. The obtained polymer **15** was a yellow powder with a yield of 0.098 g (49%). M_n^{NMR}=12,000 g/mol, M_n^{GPC}=11,000 g/mol, M_w/M_n=1.12. ^{1}H NMR (200 MHz, $CDCl_3$): δ 1.48 (br, 2H), 1.86 (br, 1H), 2.09 (br, 2H), 2.41 (br, 2H), 3.24 (br, 2H), 4.65 (s, 2H), 5.01 (br, 2H), 6.55 (br, 2H), 7.07 (br, 2H), and 7.4-8.4 (br, 9H). ^{13}C NMR (50 MHz, $CDCl_3$): δ 21.1, 29.6, 33.6, 38.5, 39.5, 40.7, 47.1, 72.9, 130.0, 131.6, 132.6, 133.5, 134.2, 135.5, 136.7, 137.6, 138.2, 140.1, 142.4, 161.8, and 180.1.

Poly-[(styrene-pyrene)-*r*-styrene)], Polymer **16**

Polymer **16** was prepared using the same procedure as that used for polymer **15** except that both styrene and monomer **5** were used together as the monomers. In a typical experiment, a 20 mL round bottom flask was charged with styrene (0.52 g, 0.50 mmol, 46 eq.), monomer **5** (0.080 g, 0.20 mmol, 19 eq.), initiator **1** (0.040 g, 1.1×10^{-2} mmol, 1 eq.), free nitroxide **2** (1.2×10^{-5} g, 5.4×10^{-5}, 0.05 eq.), acetic anhydride (5.5×10^{-6} g, 5.4×10^{-5}, 0.05 eq.) and chlorobenzene (0.8 mL) and heated to 125°C under argon. The reaction was allowed to proceed for 16 hours. Finally, the reaction mixture was diluted with 2 mL of CH_2Cl_2, and the random copolymer was precipitated into cold methanol. The polymer was further purified by repeated precipitations as outlined for polymer **12**. The precipitated solid was filtered and dried to provide a pale yellow powder. Yield: 0.12 g (20%). M_n^{NMR}=6,600 g/mol, M_n^{GPC}=7,000 g/mol, M_w/M_n=1.18. ^{1}H NMR (200 MHz, $CDCl_3$): δ 0.89 (br, 6H), 1.29 (br, 2H), 1.59 (br, 1H), 2.06 (br, 2H), 2.35 (br, 2H), 3.16 (br, 2H), 4.42 (br, 2H), 4.97 (br, 2H), 5.9-7.2 (br, 4H), and 7.4-8.3 (br, 9H). ^{13}C NMR (50 MHz, $CDCl_3$): δ 21.1, 29.6, 33.6, 38.5, 39.5, 40.6, 72.9, 130.0, 131.6, 132.6, 133.3, 134.0, 135.5, 135.8, 136.6, 138.9, 142.3, 152.2, and 180.0.

Poly-[(styrene-pyrene)-*r*-styrene)], Polymer **17**

Polymer **17** was prepared using the same procedure as the one employed in the polymer **15** except that the feed ratio of monomer **5** to styrene was 10:100 (**17**)

instead of 100:0 (**15**). Specifically, styrene (0.52 g, 0.50 mmol, 46 eq.), monomer **5** (0.20 g, 0.450 mmol, 4.6 eq.), initiator **1** (0.020 g, 0.054 mmol, 1 eq.), free nitroxide **2** (6.0×10^{-4} g, 2.7×10^{-3} mmol, 0.05 eq.), acetic anhydride (3.0×10^{-4} g, 2.7×10^{-3} mmol, 0.05 eq.) and 0.8 mL of chlorobenzene were mixed together and heated to 125°C under nitrogen overnight. The product was purified by precipitation, as outlined for polymer **12**. Yield: 0.66 g (80%). M_n^{NMR} = 12,200 g/mol, M_n^{GPC} = 11,600 g/mol, M_w/M_n = 1.22. ^{1}H NMR (200 MHz, $CDCl_3$): δ 1.27 (br, 2H), 1.67 (br, 1H), 2.05 (br, 2H), 2.35 (br, 2H), 3.23 (br, 2H), 4.40 (br, 2H), 4.89 (br, 2H), 6.0-7.3 (br, 4H), and 7.4-8.3 (br, 9H). ^{13}C NMR (50 MHz, $CDCl_3$): δ 29.6, 39.5, 40.6, 50.0, 52.8, 72.9, 131.7, 132.6, 133.6, 134.6, 134.9, 135.5, 152.2, 161.5, and 180.4.

PMMA, Polymer **19**

In a typical experiment, a flame-dried round bottom flask equipped with a magnetic stir bar was charged with CuBr (0.080 g, 0.56 mmol, 0.66 eq.) and bipyridine (0.35 g, 2.24 mmol, 2.6 eq.), and was sealed with a rubber septum. To a second round bottom flask, a mixture of initiator **19** 2-bromo-2-methyl-propionyl bromide (0.065 g, 0.28 mmol, 1 eq.), MMA (6.0 mL, 56 mmol, 200 eq.), 4 mL of H_2O, and 16 mL of DMF were added. After bubbling argon through both flasks for 30 minutes separately, the solution in the second flask was transferred to the first one via a two-headed needle under a stream of argon. Following the formation of a grey homogeneous solution, the polymerization

mixture was sealed under argon and placed in an oil bath maintained at room temperature for approximately two hours. During the polymerization the polymer was observed to precipitate. The resulting reaction mixture was filtered, and the residue was dissolved in 5 mL of THF, isolated and purified by filtration through basic Al_2O_3 on a thin layer of celite. This was followed by repeated precipitations (3 times) into methanol (200 mL). The precipitate was then collected through filtration and dried under vacuum for three days to give the desired polymer **19**, as a white powder. Typical isolated yields were 40-80% with a polydispersity of less than 1.5. Yield: 3.7 g (65%). M_n^{NMR}=9,000 g/mol, M_n^{GPC}=10,000 g/mol, M_w/M_n=1.39. ^{1}H NMR (200 MHz, $CDCl_3$): δ 0.84 (br, 3H), 1.13 (s, 6H), 1.80 (br, 2H), 3.59 (br, 3H); ^{13}C NMR (50 MHz, $CDCl_3$): δ 16.7, 19.0, 44.8, 45.1, 52.1, 52.8, 54.6, 177.2, 178.1, and 178.4.

Poly[MMA-*b*-(acrylate-pyrene)], Polymer **20**

A flame-dried 20 mL round bottom flask equipped with a stir bar was charged with CuBr (0.014 g, 0.10 mmol, 5 eq.), bypyridine (0.060 g, 0.38 mmol, 19 eq.), monomer **8** (0.033 g, 0.10 mmol, 5 eq.) and bromo-terminated polymer **19** (0.21 g, 0.02 mmol, 1 eq.). It was then sealed with a rubber septum and degassed by bubbling with argon for 30 minutes. After this, deoxygenated DMF (2 mL, after degassing with argon for 30 minutes) was added via a two-headed needle under a stream of argon. The polymerization was carried out at 50°C within twelve hours under argon atmosphere. The resulting product was purified

using the same procedure outlined for polymer **19**. Yield: 0.20 g (77%). M_n^{NMR}=11,000 g/mol, M_n^{GPC}=16,500 g/mol, M_w/M_n=1.39. ^{1}H NMR (200 MHz, $CDCl_3$): δ 0.91 (br, 3H), 1.13 (s, 6H), 1.81 (br, 2H), 3.58 (br, 3H), and 7.5-8.3 (br, 9H). ^{13}C NMR (50 MHz, $CDCl_3$): δ 16.5, 18.8, 30.3, 44.5, 44.9, 51.9, 52.6, 54.4, 124-130, 177.0, 177.9, and 178.1.

Poly{MMA-*b*-[(acrylate-pyrene)-*r*-MMA]}, Polymer **21**

Polymer **21** was prepared using the same procedure as the one employed in the polymer **20** except that the feed ratio of monomer **8** to MMA in the second block was 40:100 (**21**) instead of 100:0 (**20**). Specifically, polymer **19** (0.20 g, 0.02 mmol, 1 eq.), monomer **8** (0.033 g, 0.10 mmol, 5 eq.), CuBr (18 mg, 0.12 mmol, 6 eq.) and bipyridine (0.062 g, 0.38 mmol, 19 eq.) were added to the first flask and bubbled with argon for 30 minutes. MMA (20 μL, 0.25 mmol, 12.5 eq.), 0.4 mL of H_2O and 1.6 mL of DMF were added in the second flask and also bubbled with argon for 30 minutes. The solution in the 2nd flask was then transferred to the first one via a two-headed needle under a stream of argon. The polymerization was carried out at room temperature overnight. After 3 precipitations into MeOH, 0.035 g (13% yield) of dried polymer **21** was obtained. M_n^{NMR}=16,000 g/mol, M_n^{GPC}=15,500 g/mol, M_w/M_n=1.36. ^{1}H NMR (500 MHz, $CDCl_3$): δ 0.83 (br, 3H), 1.10 (s, 6H), 1.78 (br, 2H), 3.50 (br, 3H), and 7.1-8.8 (br, 9H). ^{13}C NMR (50 MHz, $CDCl_3$): δ 16.8, 18.9, 30.1, 44.9, 45.3, 52.3, 55.1, 124-132, 177.8, and 178.2.

Poly{MMA-*b*-[(acrylate-pyrene)-*r*-MMA]}, Polymer **22**

Polymer **22** was prepared using the same procedure as the one employed in the polymer **20** except that the feed ratio of monomer **8** to MMA in the second block was 10:100 (**22**) instead of 100:0 (**20**). Specifically, polymer **19** (0.20 g, 0.02 mmol, 1 eq.), monomer **8** (0.033 g, 0.10 mmol, 5 eq.), CuBr (0.018 g, 0.12 mmol, 6 eq.) and bipyridine (0.065 g, 0.40 mmol, 20 eq.) were added to the first flask and bubbled with argon for 30 minutes. MMA (80 μL, 1 mmol, 50 eq.), 0.4 mL of H_2O and 1.6 mL of DMF were added to the second flask and also bubbled with argon for 30 minutes. The solution in the 2nd flask was then transferred to the first one via a two-headed needle under a stream of argon. Using the same work-up procedure described for polymer **21**, 0.051 g (15%) of dried polymer **22** was obtained. M_n^{NMR}=17,500 g/mol, M_n^{GPC}=15,500 g/mol, M_w/M_n=1.26. ^{1}H NMR (200 MHz, $CDCl_3$): δ 0.90 (br, 3H), 1.19 (s, 6H), 1.89 (br, 2H), 3.58 (br, 3H), and 7.6-8.5 (br, 9H). ^{13}C NMR (50 MHz, $CDCl_3$): δ 16.5, 18.7, 30.2, 44.5, 44.9, 51.8, 54.4, 54.9, 124-130, 177.9, and 178.2.

P(*t*-BA), polymer **24**

A flame-dried round bottom flask equipped with a magnetic stir bar was charged with CuBr (98 mg, 0.68 mmol, 1 eq.), sealed with a rubber septum and bubbled with argon for 30 minutes. The 2-ethylbromopropionate initiator **25** (1.2×10^{-3} g, 0.68 mmol, 1 eq.), and *t*-BA (8.8 g, 68 mmol, 100 eq.) were added to

a second flame-dried flask and bubbled with argon for 30 minutes. The solution in the second flask was then transferred to the first flask via a two-headed needle under a stream of argon. PMDETA (0.12 g, 0.68 mmol, 1 eq.) was then added to the mixture by a gas-tight syringe. Following the formation of a green homogeneous solution, the reaction mixture was carefully deoxygenated by re-bubbling with argon for another 30 minutes to remove any dissolved oxygen and then sealed under argon. The reaction mixture was placed in an oil bath maintained at 55 °C for 2 hours. After the desired molecular weight was achieved (tested by GPC), the reaction was rapidly terminated by immersing the reaction flask in a mixture of methanol and dry ice. The polymer samples were dissolved in 10 mL of CH_2Cl_2, isolated and purified by filtration through basic Al_2O_3 on a thin layer of celite, followed by repeated precipitations into 300 mL of methanol/water (7/3 v/v) mixtures at 0°C. The precipitate was then collected through filtration and dried under vacuum to give the desired polymer **24**, as a white powder. Yield: 4.1 g (50%). M_n^{NMR}=10,000 g/mol, M_n^{GPC}=13,900 g/mol, M_w/M_n=1.29. ^{1}H NMR (200 MHz, $CDCl_3$): δ 1.26-1.60 (br, 9H), 1.80 (br, 2H), 2.22 (br, 1H), and 4.10 (q, 2H). ^{13}C NMR (50 MHz, $CDCl_3$): δ 28.0, 28.1, 41.9, 42.4, 80.3, and 174.1.

Poly[(*t*-BA)-*b*-(acrylate-pyrene)], Polymer **25**

A flame-dried round-bottom flask equipped with a magnetic stir bar was charged with polymer **24** (0.28 g, 0.02 mmol, 1 eq), monomer **8** (0.073 g, 0.22

mmol, 11 eq.), CuBr (0.014 g, 0.10 mmol, 5 eq.) and was sealed with a rubber septum. DMF (1 mL) was added to the second round-bottom flask. After bubbling both flasks with argon for 30 minutes, the solution in the second flask was then transferred to the first one via a two-headed needle under a stream of argon. PMDETA (20 μL, 0.10 mmol, 5 eq.) was then added to the mixture by a gas tight syringe. Following the formation of a green homogeneous solution, the reaction mixture was carefully deoxygenated by re-bubbling with argon for another 30 minutes to remove any dissolved oxygen and then sealed with a rubber septum under argon. The reaction mixture was placed in an oil bath maintained at 55 °C overnight. The resulting mixture was diluted with 5 mL of CH_2Cl_2, isolated and purified by filtration through basic Al_2O_3 on a thin layer of celite, followed by flash column chromatography (pure CH_2Cl_2 as eluent). This resulted in isolation of copolymer **25**, as a pale yellow solid. Yield: 0.15 g (43%). M_n^{NMR}=13,000 g/mol, M_n^{GPC}=19,400 g/mol, M_w/M_n=1.40. ^{1}H NMR (500 MHz, $CDCl_3$): δ 1.08-1.80 (br, 11H), 1.87 (br, 4H), 2.09, (br, 2H), 2.20 (br, 1H), 4.08 (br, 2H), 4.12 (q, 2H), and 7.7- 8.3 (br, 9H). ^{13}C NMR (50 MHz, $CDCl_3$): δ 28.0, 28.1, 35.9, 37.1, 37.3, 41.6, 42.0, 42.4, 80.3, 80.4, 124-130, 173.7, 174.0, and 174.1.

Poly{(*t*-BA)-*b*-[(acrylate-pyrene)-*r*-(*t*-BA)]}, Polymer **26**

Polymer **26** was prepared using the same procedure as the one employed in the polymer **25** except that the feed ratio of monomer **8** to *t*-BA in the second block was 40:100 (**26**) instead of 100:0 (**25**). Specifically, polymer **24** (0.28 g,

0.02 mmol, 1 eq.), monomer **8** (0.079 g, 0.22 mmol, 11 eq), and CuBr (0.015 g, 0.10 mmol, 5 eq.) were added to a 25 mL round bottom flask sealed with a rubber septum. To a second flask was added 1.0 mL of DMF and *t*-BA (92 μL, 0.56 mmol, 28 eq.) followed by degassing with argon for 30 minutes. Then the solution in the second flask was transferred to the first one via a two-headed needle under a stream of argon. PMDETA (20 μL, 0.10 mmol, 5 eq.) was then added to the mixture by a gas-tight syringe. After bubbling with argon for another 30 minutes, the mixture was then stirred at 55°C overnight and purified as outlined for polymer **25**. The resulting polymer **26** was a very pale yellow solid. Yield: 0.12 g (26%). M_n^{NMR}=15,000 g/mol, M_n^{GPC}=22,500 g/mol, M_w/M_n=1.33. ^{1}H NMR (500 MHz, $CDCl_3$): δ 0.8-2.0 (br, 11H), 2.09 (br, 4H), 2.29 (br, 1H), 3.13 (br, 2H), 3.98 (br, 2H), 4.18 (q, 2H), and 7.4- 8.4 (br, 9H). ^{13}C NMR (50 MHz, $CDCl_3$): δ 28.0, 28.1, 35.9, 37.2, 37.4, 41.6, 41.9, 42.0, 42.4, 80.3, 80.4, 120-135, 173.7, 173.9, and 174.1.

Poly{(*t*-BA)-*b*-[(acrylate-pyrene)-*r*-(*t*-BA)]}, Polymer **27**

Polymer **27** was prepared using the same procedure as the one employed in the polymer **25** except that the feed ratio of monomer **8** to *t*-BA in the second block was 10:100 (**27**) instead of 100:0 (**25**). Specifically, polymer **24** (0.28 g, 0.02 mmol, 1 eq.), monomer **8** (0.074 g, 0.22 mmol, 11 eq.), and CuBr (0.018 g, 0.12 mmol, 6 eq.) were added to a 25 mL round bottom flask sealed with a rubber septum. DMF (1 mL) and *t*-BA (300 μL, 2.0 mmol, 28 eq.) were added to the

second round bottom flask. After degassing both flasks with argon for 30 minutes, the solution in the second flask was transferred to the first one via a two-headed needle under a stream of argon. PMDETA (20 μL, 0.10 mmol, 5 eq.) was then added to the mixture by a gas-tight syringe. After bubbling with argon for another 30 minutes, the mixture was then stirred at 55°C overnight and purified as outlined for polymer **25**. The resulting polymer **27** was a very pale yellow solid. Yield: 0.18 g (23%). M_n^{NMR}=16,500 g/mol, M_n^{GPC}=22,400 g/mol, M_w/M_n=1.35. ^{1}H NMR (500 MHz, $CDCl_3$): δ 0.7-1.95 (br, 11H), 2.19 (br, 2H), 3.31 (br, 2H), 4.05 (br, 2H), 4.12 (q, 2H), and 7.5- 8.3 (br, 9H). ^{13}C NMR (125 MHz, $CDCl_3$): δ 14.2, 21.0, 26.4, 28.0, 28.1, 28.6, 29.6, 33.0, 34.5, 36.0, 37.4, 41.6, 42.0, 42.4, 60.3, 64.3, 73.2, 80.3, 104.1, 122.1, 123.2, 124.6, 124.8, 125.0, 125.8, 126.5, 127.2, 127.4, 128.5, 129.8, 130.9, 131.4, 136.3, 173.7, 173.9, 174.1, and 174.4.

Polymers, **28**, **29**, and **30**

To a clean 20 mL vial equipped with a stir bar was added 0.5 g of polymer **25**, polymer **26**, or polymer **27** and 10 mL of dry CH_2Cl_2. The mixture was allowed to stir for 10 minutes to dissolve the polymer. Trifluoracetic acid (3 mL) was then added. After the mixture was allowed to stir at room temperature for 12 hours, the excess TFA and CH_2Cl_2 were removed at room temperature with nitrogen gently flowing through the flask overnight. The resulting light-brown solid was dried under vacuum for three days. Yields were typically greater than

95%. ^{1}H NMR: (200 MHz, D_2O): δ 1.0-2.0 (br, 2H) and 2.24 (br, 1H). IR: 2500-4000 (br, m), 1764, 1710, and 1453 cm^{-1}.

References:

1. Iijima, S. *Nature* **1991**, *354*, 56.
2. Iijima, S.; Ichihashi, T. *Nature* **1993**, *363*, 603.
3. Ajayan, P. M. *Chem. Rev.* **1999**, *99*, 1787.
4. Ebbesen, T. W.; Ajayan, P. M. *Nature* **1992**, *358*, 220.
5. Bethune, D. S.; Kiang, C. H.; de Vries, M. S.; Gorman, G.; Savoy, R.; Vazquez, J.; Beyers, R. *Nature* **1993**, *363*, 605.
6. Thess, A.; Lee, R.; Nikolaev, P.; Dai, H.; Petit, P.; Robert, J.; Xu, C.; Lee, Y. H.; Kim, S. G.; Rinzler, A. G.; Colbert, D. T.; Scuseria, G. E.; Tomanek, D.; Fischer, J. E.; Smalley, R. E. *Science* **1996**, *273*, 483.
7. Journet, C.; Maser, W. K.; Bernier, P.; Loiseau, A.; Chapelle, M. L.; Lefrant, S.; Deniard, P.; Lee, R.; Fischer, J. E. *Nature* **1997**, *388*, 756.
8. Niyogi, S.; Hamon, M. A.; Hu, H.; Zhao, B.; Bhowmik, P.; Sen, R.; Itkis, M. E.; Haddon, R. C. *Acc. Chem. Res.* **2002**, *35*, 1105.
9. Dujardin, E.; Ebbesen, T. W.; Krishnan, A.; Treacy, M. M. J. *Adv. Mater.* **1998**, *10*, 1472.
10. Ajayan, P. M.; Lambert, J. M.; Bernier, P.; Barbedette, L.; Colliex, C.; Planeix, J. M. *Chem. Phys. Lett.* **1993**, *215*, 509.
11. Guo, T.; Nikolaev, P.; Thess, A.; Colbert, D. T.; Smalley, R. E. *Chem. Phys. Lett.* **1995**, *243*, 49.
12. Wilder, I. W. G.; Venema, L. C.; Rinzler, A. G.; Smalley, R. E.; Dekker, C. *Nature* **1998**, *391,* 59.
13. Odom, T. W.; Huang, J. L.; Kim, P.; Lieber, C. M. *Nature* **1998**, *391*, 62.
14. Li, F.; Cheng, H. M.; Bai, S.; Su, G.; Dresselhaus, M. S. *App. Phys. Lett.* **2000**, *77*, 3161.
15. Yu, M. F.; Files, B. S.; Arepalli, S.; Ruoff, R. S. *Phys. Rev. Lett.* **2000**, *84*, 5552.
16. Hone, J.; Batlogg, B.; Benes, Z.; Johnson, A. T.; Fischer, J. E. *Science* **2000**, *289*, 1730.

17. Wong, E. W.; Sheehan, P. E.; Lieber, C. M. *Science* **1997**, *277*, 1971.
18. Falvo, M. R.; Clary, C. J.; Taylor, R. M.; chi, V.; Brooks, F. P.; Washburn, S.; Superfine, R. *Nature* **1997**, *389*, 582.
19. Baughman, R. H.; Zakhidov, A.; de Heer, W. A. *Science* **2002**, *297*, 787.
20. Dai, H. *Acc. Chem. Res.* **2002**, *35*, 1035.
21. Tombler, T.; Zhou, C.; Alexeyev, L.; Kong, J.; Dai, H.; Liu, L.; Jayanthi, C. S.; Tang, M.; Wu, S. Y. *Nature* **2000**, *405*, 769.
22. Heer, W. A.; Chatelain, A.; Ugaarte, D. A. *Science* **1995**, *270*, 1179.
23. Fan, S.; Chapline, M. G.; Franklin, N. R.; Tombler, T. W.; Cassell, A. M.; Dai, H. *Science* **1999**, *283,* 512.
24. Tans, S.; Verschueren, A.; Dekker, C. *Nature* **1998**, *393*, 49.
25. Collins, P. G.; Arnold, M. S.; Avouris, P. *Science* **2001**, *292*, 706.
26. Kong, J.; Franklin, N. R.; Zhou, C.; Chapline, M. G.; Peng, S.; Cho, K.; Dai, H. *Science* **2000**, *287*, 622.
27. Collins, P. G.; Bradley, K.; Ishigami, M.; Zettl, A. *Science* **2000**, *287*, 1801.
28. Balaboine, F.; Schultz, P.; Richard, C.; Mallouh, V.; Ebbessen, T. W.; Mioskowski, C. *Angew. Chem. Int. Ed.* **1999**, *38*, 1912.
29. Hu, J.; Odom, T. W.; Lieber, C. M. *Acc. Chem. Res.* **1999**, *32*, 435.
30. Ebbesen, T. W.; Ajayan, P. M. *Nature* **1992**, *358*, 16.
31. Terrones, M.; Grobert, N.; Olivares, J.; Zhang, J. P.; Terrones, H.; Kordatos, K.; Hsu, W. K.; Hare, J. P.; Townsend, P. D.; Prassides, K.; Cheetham, A. K.; Kroto, H. W.; Walton, D. R. M. *Nature* **1997**, *388*, 52.
32. Jose-Yacaman, M.; Miki-Yoshida, M.; Rendon, L.; Santiesteban, T. G. *Appl. Phys. Lett.* **1993**, *62*, 202.
33. Ivanov, V.; Nagy, J. B.; Lambin, P.; Lucas, A.; Zhang, X. B.; Zhang, X. F.; Bernaerts, D.; Van Tendeloo, G.; Amelinckx, S.; Van Landuyt, J. *Chem. Phys. Lett.* **1994**, *223*, 329.
34. Ren, Z. F.; Huang, Z. P.; Xu, J. W.; Wang, J. H.; Bush, P.; Siegal, M. P.; Provencio, P. N. *Science* **1998**, *282*, 1105.

35. Pan, Z. W.; Xie, S. S.; Chang, B. H.; Wang, C. Y.; Lu, L.; Liu, W.; Zhou, W. Y.; Li, W. Z.; Qian, L. X. *Nature* **1998**, *394*, 631.
36. Nikolaev, P.; Bronikowski, M. J.; Bradley, R. K.; Rohmund, F.; Colbert, D. T.; Smith, K. A.; Smalley, R. E. *Chem. Phys. Lett.* **1999**, *313*, 91.
37. Rao, C. N. R.; Govindaraj, A.; Sen, R.; Satishkumar, B. C. *Mater. Res. Innovations* **1998**, *2*, 128.
38. Rao. C. N. R.; Govindaraj. A. *Acc. Chem. Res.* **2002**, *35*, 998.
39. Chen, J.; Hamon, M. A.; Hu, H.; Chen, Y.; Rao, A. M.; Eklund, P. C.; Haddon, R. C. *Science* **1998**, *282*, 95.
40. Hirsch, A. *Angew. Chem. Int. Ed.* **2002**, *41*, 1853.
41. Holzinger, M.; Vostrowsky, O.; Hirsch, A.; Hennrich, F.; Kappes, M.; Weiss, R.; Jellen, F. *Angew. Chem. Int. Ed.* **2001**, *40*, 4002.
42. Chen, Y.; Haddon, R. C.; Fang, S.; Rao, A. M.; Eklund, P. C.; Lee, W. H.; Dickey, E. C.; Grulke, E. A.; Pendergrass, J. C.; Chavan, A.; Haley, B. E.; Smalley, R. E. *J. Mater. Res.* **1998**, *13*, 2423.
43. Mickelson, E. T.; Huffman, C. B.; Rinzler, A. G.; Smalley, R. E.; Hauge, R. H.; Margrave, J. L. *Chem. Phy. Lett.* **1998**, *296*, 188.
44. Bahr, J. L.; Yang, J.; Kosynkin, D. V.; Bronikowski, M. J.; Smalley, R. E.; Tour, J. M. *J. Am. Chem. Soc.* **2001**, *123*, 6536.
45. Georgakilas, V.; Kordatos, K.; Prato, M.; Guldi, D. M.; Holzinger, M.; Hirsch, A. *J. Am. Chem. Soc.* **2002**, *124*, 760.
46. Coleman, K. S.; Bailey, S. R.; Fogden, S.; Green, M. L. H. *J. Am. Chem. Soc.* **2003**, *125*, 8722.
47. Chen, Y.; Chen, J.; Hu, H.; Hamon, M. A.; Itkis M. E.; Haddon, R. C. *Chem. Phys. Lett.* **1999**, *299*, 532.
48. Hamon, M. A.; Chen, J.; Hu, H.; Chen, Y.; Itkis, M. E.; Rao, A. M.; Eklund, P. C.; Haddon, R. *C. Adv. Mater.* **1999**, *11*, 834.
49. Riggs, J. E.; Guo, Z.; Carroll, D. L.; Sun, Y. P. *J. Am. Chem. Soc.* **2000**, *122*, 5879.

50. Sun, Y. P.; Fu, K.; Lin, Y.; Huang, W. *Acc. Chem. Res.* **2002**, *35*, 1096.
51. Nguyen, C. V.; Delzeit, L.; Cassell, A. M.; Li, J.; Han, J.; Meyyappan, M. *Nano Lett.* **2002**, *2*, 1079.
52. Hazani, M.; Naaman, R.; Hennrich, F.; Kappes, M. M. *Nano Lett.* **2003**, *3*, 153.
53. Nakashima, N.; Tomonari, Y.; Murakami, H. *Chem. Lett.* **2002**, 638.
54. Islam, M. F.; Rojas, E.; Bergey, D. M.; Johnson, A. T.; Yodh, A. G. *Nano Lett.* **2003**, *3*, 269.
55. Chen, J.; Rao, A. M.; Lyuksyutov, S.; Itkis, M. E.; Hamon, M. A.; Hu, H.; Cohn, R. W.; Eklund, P. C.; Colbert, D. t.; Smalley, R. E.; Haddon, R. C. *J. Phys. Chem. B.* **2001**, *105*, 2525.
56. Curran, S. A.; Ajayan, P. M.; Blau, W. J.; Carroll, D. L.; Coleman, J. N.; Dalton, A. B.; Davey, A. P.; Drury, A.; McCarthy, B.; Maier, S.; Strevens, A. *Adv. Mater.* **1998**, *10*, 1091.
57. Curran, S.; Davey, A. P.; Coleman, J. N.; Dalton, A. B.; McCarthy, B.; Maier, S.; Drury, A.; Gray, D.; Brennan, M.; Ryder, K.; Lamy de la Chapelle, M.; Journet, C.; Bernier, P.; Byrne, H. J.; Carroll, D.; Ajayan, P. M.; Lefrant, S.; Blau, W. *Synth. Met.* **1999**, *103*, 2559.
58. Coleman, J. N.; Dalton, A. B.; Curran, S.; Rubio, A.; Davey, A. P.; Drury, A.; McCarthy, B.; Lahr, B.; Ajayan, P. M.; Roth, S.; Barklie, R. C.; Blau W. J. *Adv. Mater.* **2000**, *12*, 213.
59. McCarthy, B.; Coleman, J. N.; Czerw, R.; Dalton, A. B.; Carroll, D. L.; Blau, W. J. *Synth. Met.* **2001**, *121*, 1225.
60. Panhuis, M.; Munn, R. W.; Blau, W. J. *Synth. Met.* **2001**, *121*, 1187.
61. Dalton, A. B.; Stephan, C.; Coleman, J. N.; McCarthy, B.; Ajayan, P. M.; Lefrant, S.; Bernier, P.; Blau, W. J.; Byrne H. J. *J. Phys. Chem. B*, **2000**, *104*, 10012.
62. Chen, R. J.; Zhang, Y.; Wang, D.; Dai, H. *J. Am. Chem. Soc.* **2001**, *123*, 3838.

63. O'Connell, M. J.; Boul, P.; Ericson, L. M.; Huffman, C.; Wang, Y. H.; Haroz, E.; Kuper, C.; Tour, J.; Ausman, K. D.; Smalley, R. E. *Chem. Phys. Lett.* **2001**, *342*, 265.

64. Star, A.; Stoddart, J. F.; Steuerman, D.; Diehl, M.; Boukai, A.; Wong, E. W.; Yang, X.; Chung, S. W.; Choi, H.; Heath, J. R. *Angew. Chem. Int. Ed.* **2001**, *40*, 1721.

65. Steuerman, D. W.; Star, A.; Narizzano, R.; Choi, H.; Ries, R. S.; Nicolini, C.; Stoddart, J. F.; Heath. J. R. *J. Phys. Chem. B.* **2002**, *106*, 3124.

66. Star, A.; Stoddart, J. F. *Macromolecules* **2002**, *35*, 7516.

67. Diez-Barra, E.; Garcia-Martinez, J. C.; Merino, S.; Rey, R.; Rodriguez-Lopez, J.; Sanchez-Verdu, P.; Tejeda, J. *J. Org. Chem.* **2001**, *66*, 5664.

68. Meier, H.; Lehmann, M.; Kolb, U. *Chem. Eur. J.* **2000**, *6*, 2462.

69. Meier. H.; Lehmann, M. *Angew. Chem. Int. Ed.* **1998**, *37*, 643.

70. Maddux, T. M.; Yu, L. *J. Am. Chem. Soc.* **1997**, *119*, 9079.

71. Discher, B. M.; Won, Y. Y.; Ege, D. S.; Lee, J. C. M.; Bates, F. S.; Discher, D. E.; Hammer, D. A. *Science* **1999**, *284*, 1143.

72. Bütün, V.; Wang, X. S.; Banez, M. V. D. P.; Robinson, K. L.; Billingham, N. C.; Armes, S. P. *Macromolecules* **2000**, *33*, 1.

73. Thurmond, K. B., II; Remsen, E. E.; Kowalewski, T.; Wooley, K. L. *Nucleic Acids Res.* **1999**, *27*, 2966.

74. Wooley, K. L. *J. Polym. Sci. Part A: Polym. Chem.* **2000**, *38*, 1397.

75. Huang, H.; Remsen, E. E.; Kowalewski, T.; Wooley, K. L. *J. Am. Chem. Soc.* **1999**, *121*, 3805.

76. Szwarc, M. *Adv. Polym. Sci.* **1960**, *2*, 275.

77. Miyamoto, M.; Sawamoto, M.; Higashimura, T. *Macromolecules* **1984**, *17*, 265.

78. Benoit, D.; Chaplinski, V.; Braslau, R.; Hawker, C. J. *J. Am. Chem. Soc.* **1999**, *121*, 3904.

79. Hawker, C. J.; Barclay, G. G.; Dao, J. *J. Am. Chem. Soc.* **1996**, *118*, 11467.

80. Hawker, C. J.; Barclay, G. G.; Orellana, A.; Dao, J.; Devonport, W. *Macromolecules* **1996**, *29*, 5245.
81. Matyjaszewski, K.; Patten, T. E.; Xia, J. *J. Am. Chem. Soc.* **1997**, *119*, 674.
82. Matyjaszewski, K.; Coca, S.; Gaynor, S. G.; Wei, M.; Woodworth, B. E. *Macromolecules* **1997**, *30*, 7348.
83. Matyjaszewski, K.; Coca, S.; Gaynor, S. G.; Wei, M.; Woodworth, B. E. *Macromolecules* **1998**, *31*, 5967.
84. Matyjaszewski, K.; Nakagawa, Y.; Jasieczek, C. B. *Macromolecules* **1998**, *31*, 1535.
85. Sawamoto, M.; Kamigaito, M. *J Macromol. Sci. Pure Appl. Chem.* **1997**, *34*, 1803.
86. Chiefari, J.; Chong, Y. K.; Ercole, F.; Krstina, J.; Jeffery, J.; Le, T. P. T.; Mayadunne, R. T. A.; Meijs, G. F.; Moad, C. L.; Moad, G.; Rizzardo, E.; Thang, S. H. *Macromolecules* **1998**, *31*, 5559.
87. Chong, Y. K.; Le, T. P. T.; Moad, G.; Rizzardo, E.; Thang, S. H. *Macromolecules* **1999**, *32*, 2071.
88. Mayadunne, R. T. A.; Rizzardo, E.; Chiefari, J.; Chong, Y. K.; Moad, G.; Thang, S. H. *Macromolecules* **1999**, *32*, 6977.
89. Mayadunne, R. T. A.; Rizzardo, E.; Chiefari, J.; Krstina, J.; Moad, G.; Postma, A.; Thang, S. H. *Macromolecules* **2000**, *33*, 243.
90. Percec, V.; Barboiu, B.; Bera, T. K.; Van Der Sluis, M.; Grubbs, R. B.; Frechet, J. M. J. *J. Polym. Sci. Part A: Polym. Chem.* **2000**, 38, 4776.
91. Matyjaszewski, K.; Xia, J. *Chem. Rev.* **2001**, 101, 2921.
92. Hawker, C. J.; Bosman, A. W.; Harth, E. *Chem. Rev.* **2001**, 101, 3661.
93. Kamigaito, M.; Ando, T.; Sawamoto, M. *Chem. Rev.* **2001**, 101, 3689.
94. Benoit, D.; Chaplinski. V.; Braslau, R.; Hawker, C. J. *J. Am. Chem. Soc.* **1999**, *121*, 3904.
95. Georges. M. K.; Veregin, R. P. N.; Kazmaier, P. M.; Hamer, G. K.; Saban, M. *Macromolecules* **1994**, *27*, 7228.

96. Malmstrom, E. E.; Miller, R. D.; Hawker, C. J. *Tetrahedron* **1997**, *53*, 15225.
97. Smalley, R. E. *Chem. Comm.* **2001**, 193.
98. Yao, L. Braidy, N.; Batten, G. A.; Adronov, A. *J. Am. Chem. Soc.* **2003**, in press.